Effect of Surface Modifications on the Fatigue Performance of Additively Manufactured Ti-6Al-4V Miniature Tensile Specimens Used in Lattices for Orthopaedic Implants

Master Thesis

Patrik Markovic

Advisors

Prof. Dr. E. Mazza, Dr. E. Hosseini

Institute of Mechanical Systems, ETH Zürich
Experimental Continuum Mechanics, Empa

March 30, 2021

i

Abstract

Fully solid metal implants used in orthopaedic applications suffer from stress shielding effects, causing periprosthetic bone loss and leading to complications, implant failure and higher risk for revision surgery. Emerging from a stiffness mismatch between adjacent bone and implant, stress shielding effects can be reduced by tailoring the aparent elastic modulus of porous implants to meet the mechano-biological requirement imposed by Wolff's law.

Porous implants can be realised by the incorporation of periodic micro-architected cellular materials, such as lattice structures, using additive manufacturing technology. The mechanical response of tetrahedron-based Ti-6Al-4V lattices, produced by selective laser melting, were previously shown to meet a similar stiffness response to the one of native bone. However, cyclic testing revealed; emerging from structurally related notches at nodes and arising from the poor surface quality as well as internal defects associated with additive manufacturing process, high stress concentrations act on individual struts and adversely affect the fatigue performance of the lattice structures.

In this work, the effect of different surface modifications were investigated on the fatigue performance improvement of selectively laser melted Ti-6Al-4V miniature tensile specimens, representing individual trusses of lattice structures. Surface modification processes involve: 1) surface smoothing of the specimens applied by chemical etching using Kroll's etchant, 2) specimen dip coating from a PMMA solution and 3) sol-gel derived TiO_2 dip coating of the specimens.

The fatigue results were interpreted with the help of optical microscopy observations and FE analysis. Furthermore, each surface modification process was applied on lattice structures and assessed in terms of feasibility. The investigation revealed; chemical etching was highly effective in improving fatigue endurance of struts but challenges arose for the application on lattices as the homogeneity of the etching effect is impaired within internal parts. The effect of the PMMA coating on the improvement in fatigue response of the struts was only marginal. In particular, its application on the lattice structures via spin coating was unsuccessful due to poor wettability of the PMMA solution. The TiO_2 coating enhanced the fatigue performance of the strut specimens, and furthermore, its application on lattices via spin coating was observed to be feasible. In spite of optimisation methods, cracking of the TiO_2 coating could not be avoided, which may arose from capillary activities induced by the rough and uneven surface of the strut specimens. Optimised deposition methods are required for crack-free coatings.

This preliminary investigation provides a fundamental basis for further research to improve the fatigue properties of selectively laser melted lattice structures by post-process surface modification treatments.

Acknowledgment

First of all, I want to thank Prof. Dr. Edoardo Mazza for giving me the opportunity to do my master thesis in the Experimental Continuum Mechanics laboratory and for the mentoring as tutor during my master studies.
Foremost, I wish to express my gratitude to Dr. Ehsan Hosseini, for his continuous support, guidance and immense knowledge. I appreciate all the advice and the inspiring discussions during the last six months.

Another thanks goes to all people of the Experimental Continuum Mechanics Group, especially Serjosha who helped me with the biaxial MTS machine, Xiaolong and Jian who both performed SEM images for me, Xi who helped me with the FDM printing and Dr. Kilian Schillai for the interesting discussions.
A special thanks goes to the people of the Superinsulation Materials Group of Empa for the provided infrastructure and for the recommendation with regard to coating.
Furthermore, I thank Dr. Hans Rudolf Elsener for the applied heat treatments with the vacuum furnace.

I am also grateful to my friends, Silvan and Philipp, who supported me mentally during my studies and provided laser cutting and 3D printing, respectively, for my master thesis.

Last but not least, I want to express my sincere gratitude to my family. I am deeply in debt to my wife, Rovina. She is a continuous source of happiness for me and allowed me to finish my studies with all her encouragement and support.

Contents

1. Introduction

1.1. Motivation

For many years, metallic biomaterials have been implanted into the human body as prostheses to replace joints, long bones and skull plates. Currently, titanium and it's alloys, especially Ti-6Al-4V (Ti64), are the most favoured implant materials in the field of trauma and orthopaedic surgery. Despite the fact that Ti-6Al-4V was originally developed for aerospace applications, it led into the biomedical industry due to its outstanding properties, such as its high strength, high fracture toughness, excellent corrosion resistance and biocompatibility [1].

In spite of the progress in quality of biomaterials used in orthopaedic applications, patients are still suffering from serious problems in long-term usability. One of the major issues is peri-implant bone resorption that is caused by stress shielding effects [2]. Stress shielding originates from the mismatch in elastic modulus between currently used implants and the surrounding native bone [3]. Especially in load-bearing applications, stress shielding becomes detrimental such as in hip implants. The stiff prosthesis absorbs a substantial part of the stresses when the hip is loaded during gait or other physical activities. This leads to insufficient loading of the adjacent bone, and eventually, results in periprosthetic bone loss, as highlighted in figure 1.1. The resorption of surrounding bone can lead to implant loosening and increased risk of peri-implant bone fracture. Thus, a subsequent revision surgery is required for over 15% of hip implants [4], and on top of it, the bone loss around the prosthesis increases its complexity and failure rate [5, 6].
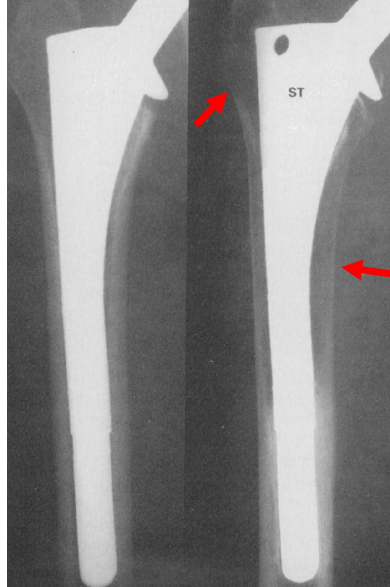
Figure 1.1: X-ray image demonstrating the pronounced peri-implant bone loss; immediate postoperative x-ray image (on the left side) in comparison to the x-ray image two years after surgery (on the right side) of a sixty-six-year-old female patient [7].

Based on extrapolation of the increases over the past decade, the demand for primary total hip arthroplasties is estimated to grow by 174% for the year 2030 [4]. Furthermore, the demand for hip revision procedures is projected to double by the year 2026 [4]. Considering these projected increases and the elevated revision complexity imposed by periprosthetic bone loss, the research and development of new or improved biomaterials become of great importance.

One approach to reduce bone loss secondary to stress shielding involves the development of biomaterials that provide a similar elastic modulus to the native bone, meeting the mechano-biological requirement imposed by Wolff's law [8]. Recent methodologies involve porous materials whose elastic modulus can be tailored by the level of introduced porosity, reconciling the elastic property mismatch between implant and bone [9]. Porous implants can be realised by the incorporation of periodic micro-architected cellular materials using additive manufacturing technology [10], as shown in figure 1.2.
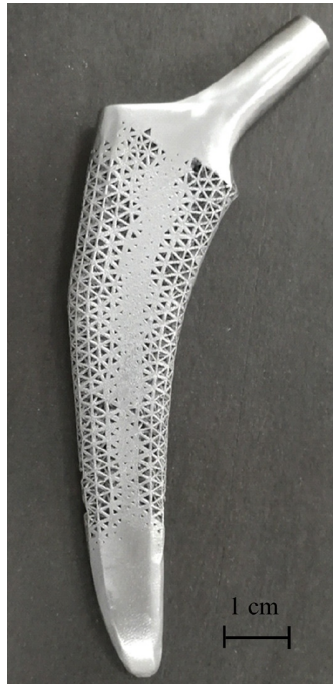
Figure 1.2: Titanium alloy implant with optimized lattice architecture built via additive manufacturing [10].

In addition, open-cell porous structures consist of large interconnected volume which promotes bone ingrowth into the pores and enables better osseointegration [11, 12]. An improved bone ingrowth provides not only a better interlocking for implant fixation, but also it creates a bone-implant-system which enables stresses to be transferred from the implant to the native bone, leading to long-term stability [13].

Porous biomaterials can be fabricated using traditional methods such as; 1) direct metal foaming, 2) powder metallurgy, and 3) vapor deposition. However, they provide only limited design freedom; 1) and 2) produce only random pore distribution whereas 3) can only produces uniform arrangements of cells [14].

The recent progress in additive manufacturing (AM) enables the realisation of near-net shape component directly from CAD models. Compared to conventional fabrication methods, AM is not subtractive, but is characterized by adding material in a layer-by-layer fashion. AM brings a large design freedom and facilitates the fabrication of porous parts with a controlled pore morphology, e.g. implants with controlled gradients of porosity depending on the anatomical location.
Several processes for various materials are included in AM. For metals, there are three broad categories of AM systems such as powder bed systems, powder feed systems and wire feed systems. Figure 1.3 illustrates the schematic process of selective laser melting (SLM). The laser is programmed to selectively transfer heat to the surface of the pow-

der layer, thereby sintering and melting the particles to form the desired shape. After powder consolidation, the build platform is lowered and an additional layer is spread on top. Repeating this process yields a solid three-dimensional component [15].
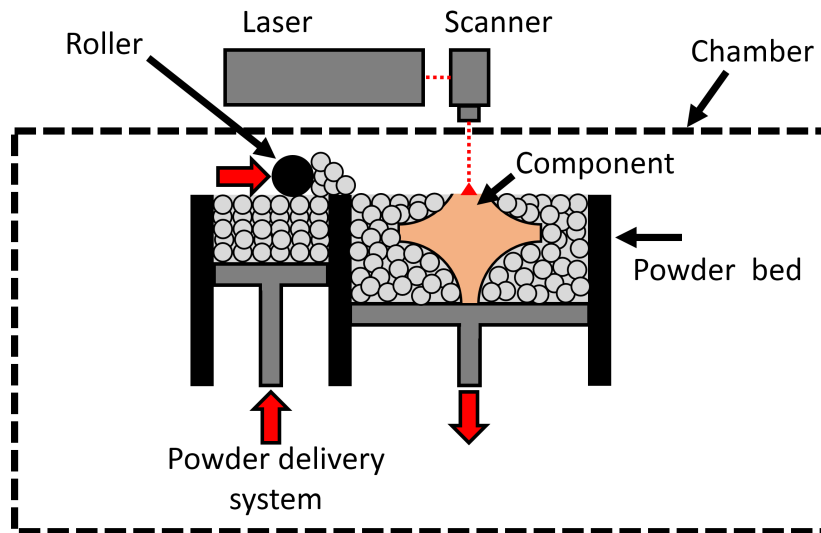
Figure 1.3: Generic illustration of a laser powder bed system.

AM provides the capability of fabricating parts with inherently complex geometries such as architected cellular materials with a periodic arrangement, consisting of struts and nodes. These so-called lattice structures are characterized by a three-dimensional network of connected unit cells and can be determined by a small number of design parameters. Thus, their mechanical properties can be characterized as a function of their morphological parameters. In order to address the problem of bone loss secondary to stress shielding, such lattice structures can be incorporated into orthopaedic implants, yielding a porous prosthesis with a well defined microarchitecture. However, lattices suffer from poor fatigue properties which limit their use for load-bearing applications; hence, further research addressing key challenges related to mechanical integrity of the printed lattices is required [16].

In collaboration with the Swiss Federal Institute of Technology Zürich (ETH Zürich) and the McGill University, the High Temperature Integrity Group of the Swiss Federal Laboratories for Material Science & Technology (Empa) is running a project involving the meso- and macro-scale mechanical integrity analysis of Ti-6Al-4V AM lattice structures for load-bearing applications with the following main objectives:

- Understanding the anisotropy and size dependency of the AM Ti-6Al-4V response

- Investigating the fatigue response of AM Ti-6Al-4V

- Development of an efficient numerical tool for mechanical assessment of lattice structures

1.2. Initial situation

This work is a based on previous contributions by Fürer [17], Thalmann [18], Rob-mann [19], Greenfeld [20], Gillmann [21], and Ghedalia [22] and can be considered as continuation. The initial design of the lattice structure consists of a tetrahedral-based unit cell, which is characterized by a nominal unit length of 1.19 mm and a nominal strut diameter of 200 μm, yielding a nominal porosity of 75%.
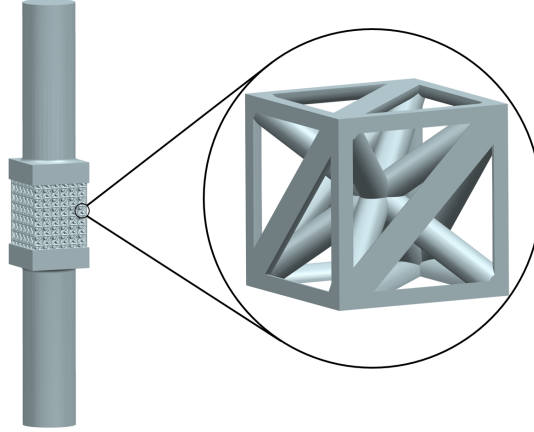
Figure 1.4: Initial design of the tetrahedon-based lattice structure.

Previously, the mechanical performance of the lattice structure was investigated with respect to tensile and fatigue properties using a load ratio of R=0.1 [17]. The results are summarized in table 1.1, where the fatigue ratio is defined as the following:

$$\text{Fatigue ratio} = \frac{\text{Fatigue strength}}{\text{Ultimate tensile strength}}. \tag{1.1}$$

Table 1.1: Previous results from static and cyclic mechanical investigations of lattices performed at a load ratio of R=0.1 compared to values from literature for cortical bone [23], bulk AM Ti-6Al-4V [24] and wrought Ti-6Al-4V [25].

Material	Elastic modulus [GPa]	Fatigue ratio at 10^6 cycles [-]
Raw Ti-6Al-4V lattice [17]	10.7	0.05
Etched Ti-6Al-4V lattice [17]	9.3	0.05
Epoxy-reinforced Ti-6Al-4V lattice [17]	14.6	0.09
Cortical bone [23]	15-17	-
Bulk AM Ti-6Al-4V [24]	109	0.2
Wrought Ti-6Al-4V [25]	-	0.26

The static mechanical performance revealed an elastic modulus for raw lattices similar to bone, thus addressing the mechano-biological requirement. However, the response in fatigue of the same lattice group performed poorly. The fatigue ratio of raw lattice samples withstood only 5% of their ultimate tensile strength at 10^6 cycles which is considerably lower compared to the fatigue ratio of bulk AM [24] or wrought Ti-6Al-4V [25]. This is a clear limitation of lattice structures and requires further research in order to enable their use in load-bearing applications.

1.3. Theory of fatigue

The following part about fatigue is based on Schivje's book "Fatigue of Structures and Materials" [26]. In general, the fatigue life consists of two periods; the crack initiation period and the crack growth period, as depicted in figure 1.5. Furthermore, the dominating factor for each period is highlighted.
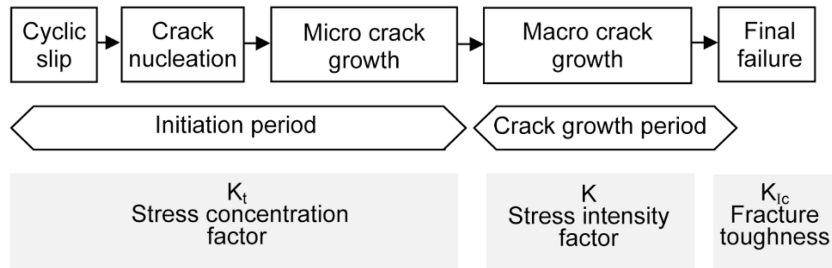
Figure 1.5: Different phases of fatigue life and relevant factors [26].

In the first phase, crack initiation is a consequence of cyclic slip which is characterised by plastic deformation along so-called slip planes. Plastic deformation occurs even at nominal stress levels significantly below the yield strength. In particular within the root of notches, stress concentrations are generated, exceed the yield strength and lead to local plastic deformation. For each consecutive cycle, the stress in the slip plane will increase and plastic deformation will accumulate until cyclic slips end up in nucleation of micro cracks. Thus, the following holds:

"In the crack initiation period, fatigue is a material surface phenomenon." [26]

As a consequence, the surface condition highly affects the crack nucleation and the dominating factor within the crack initiation period is the stress concentration factor. This parameter reflects the surface condition based on geometric values and is defined as:

$$K_t = \frac{\sigma_{max}}{\sigma_{nominal}}. \tag{1.2}$$

Within the second phase, micro cracks cause inhomogeneous stress distributions on a microlevel with a stress concentration at the tip of the crack. How fast the crack will

grow depends on the crack growth resistance of the material. Micro crack growth is based on cyclic plasticity where barriers such as grain boundaries can imply thresholds for crack growth. It should be noted that surface roughness and other surface conditions do not affect the crack growth anymore. Thus, it holds:

"Crack growth resistance when the crack penetrates into the material depends on the material as a bulk property. Crack growth is no longer a surface phenomenon."[26]

Within the crack growth period, the concept of a stress concentration factor K_t does not hold anymore. Instead, the stress intensity factor K is used for predictions on crack growth and represents the dominant factor within the crack growth period.
In figure 1.6, crack growth curves are illustrated and the crack growth development is shown as a function of the percentage of the fatigue life consumed.
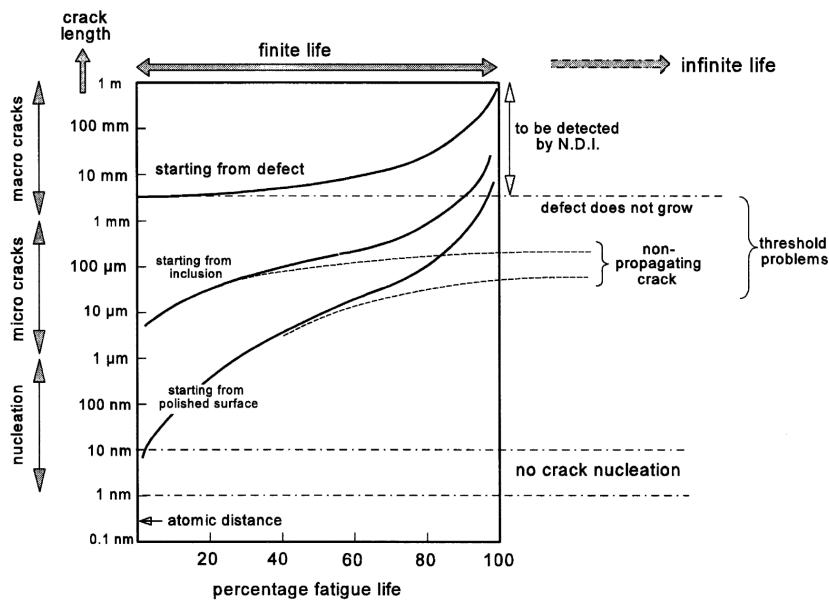
Figure 1.6: Different scenarios of fatigue crack growth [26].

Three curves are shown in figure 1.6, all starting in the crack initiation period but with different initial crack lengths. The middle and lower curve show that the major portion of the finite fatigue life is spent with the nucleation of macro cracks. As a consequence, surface effects are of great importance for fatigue life, especially in the high cycle fatigue domain [26].

1.4. Fatigue of SLM Ti-6Al-4V

Despite the capability of AM to fabricate components with a high level of complexity, the current state-of-the art of AM is is still suffering from intrinsic limitations and challenging

drawbacks. Due to the intense and high localized heat input on the powder, the final components in general include:

- Heterogeneous microstructure [27]

- Residual stresses [28]

- Internal defects within the component (porosity) [29]

- Poor surface morphology [30]

These drawbacks have a negative impact on the mechanical properties of the component especially on the fatigue strength [16, 31]. The fatigue strength becomes indispensably important for load-bearing implants, in particular for hip implants, as these prostheses have to withstand the periodic nature of the human gait [32]. Both, internal defects as well as the detrimental surface morphology were found previously in the lattices and they are associated with the poor fatigue performance of the lattices.

1.4.1. Microstructure and residual stresses

Associated with the AM process, the high solidification rate and temperature gradients in Ti-6Al-4V generate metastable, very fine and strongly textured martinsitic α' phase. In general, microstructural properties, such as grain boundaries, impede local plastic deformation along the slip plane and promote barriers for crack growth [26]. The as-built fine microstructure of SLM Ti-6Al-4V results in high strength but the presence of α' martensite limits its ductility. Additional heat treatment below 900°C leads to reduced dislocation densities and a coarser as well as uniform $\alpha+\beta$ lamellar structure, inducing higher ductility at the cost of reduced strength [33]. Thus, there is a trade-off between strength and ductility enabling the fine-tuning of mechanical properties upon heat treatment according to the desired application. Frkan et al. [34] revealed higher fatigue strength for SLM Ti6-Al-4V heat treated at 900°C compared to heat treatment at 740°C, which may be due to improved ductility.

Furthermore, the combination of high temperature gradients and fast solidification promotes the generation of residual stresses within the parts. Especially, tensile residual stresses upon AM process are unfavoured and negatively affect the fatigue performance as they can reach a considerable amount of the yield strength. Post-process heat treatments can reduce residual stresses to a negligible level as shown by Leuders et al. [35]. Thus when dealing with as-built surfaces, heat treatment of Ti-6Al-4V specimens show some fatigue-improving effect. But in the presence of high stress concentrations imposed by the surface quality, heat treatment alone is not sufficient to reach similar fatigue properties compared to wrought Ti-6Al-4V. Internal defects and the surface roughness act as stress raisers and have a significant detrimental effect on the fatigue performance [36]. As the lattices used in the previous work [17] underwent a stress relief heat treatment, the focus with respect to fatigue improvement is laid on stress raisers within the lattice.

1.4.2. Internal defects

There are two types of uncontrolled internal defects that prevail in AM parts; spherical type pores filled with gas and lack of fusion pores. Despite optimized SLM parameters, Kasperovich et al. [30] reported a porosity of 0.08% in SLM Ti-6Al-4V components. These defects act as crack nucleation sites and highly affect the fatigue life. Hot isostatic pressing (HIP) is a promising post-process treatment that combines high temperature and high pressure. It allows not only to remove residual stresses and to reach high ductility, but also to fuse internal lack of fusion defects. Kasperovich et al. reported reduced porosity levels of 0.012% upon HIP treatment [30]. However, not all manufacturers provide HIP treatment. In particular, the Ti-6Al-4V specimens used within this and previous works underwent a conventional heat treatment. Thus, internal defects were found in both strut and lattice specimens [19, 20], as shown in figure 1.7.
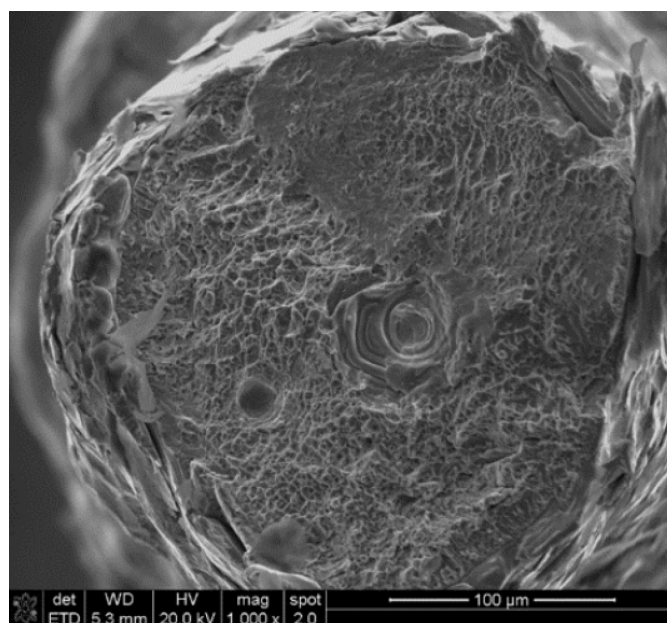
Figure 1.7: SEM image of a strut sample with internal defects [19].

In particular, internal defects act as stress raisers and promote crack nucleation [30, 35, 36] from the internal part of the strut, hence negatively affecting the fatigue performance of the lattice structures.

1.4.3. Surface morphology

In general, the poor surface quality of SLM builds is attributed to the characteristics associated with powder-based AM process and results from: [36, 37]

1. Surface asperity in microscale that is created by the physical interaction between melting process and metal powder. Within this work this is referred to as surface roughness.

2. Wave-like features reflecting the stair-step effect related to track width and hatch spacing of the AM process. Within this work this is referred to as waviness.

3. Adherence of partially melted particles on the part surface.

4. Surface defects involving open pores and incompletely melted regions due to either insufficient power or overheating of the melt pool.

Wycisk et al. [38] reported an endurance limit of 210 MPa for as-built and 500 MPa for machined SLM Ti-6Al-4V specimens, both heat-treated. This shows the detrimental effect of the surface condition on the fatigue life. The above mentioned surface characteristics are also found in the used lattice and strut specimens, as shown in figures 1.8-1.9.
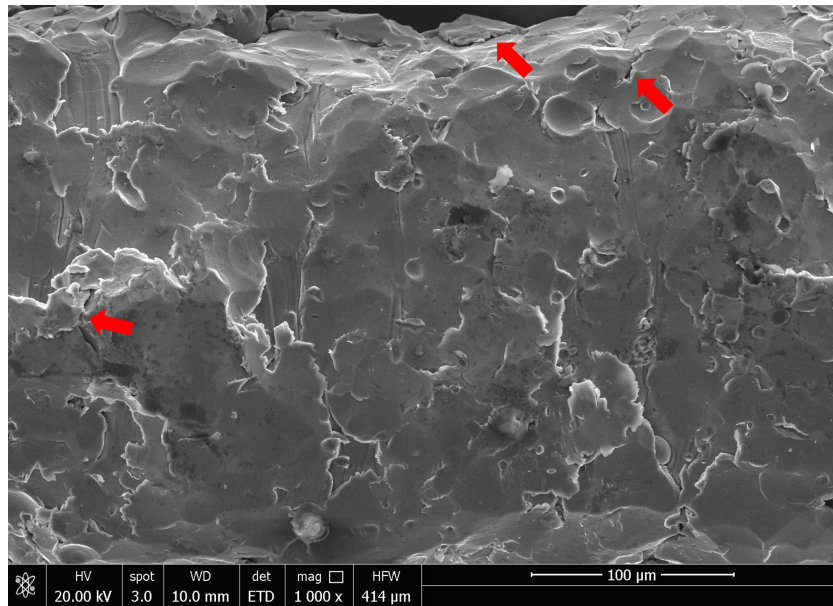
Figure 1.8: SEM image of a strut specimen showing the microlevel roughness. Furthermore, incomplete fusion defects on the surface are highlighted.

In figure 1.8, the microscale roughness and surface defects are visible on the surface of a SLM Ti-6Al-4V strut. These act as crack nucleation sites and promote a faster crack growth.

<div align="center">(a)   (b)</div>
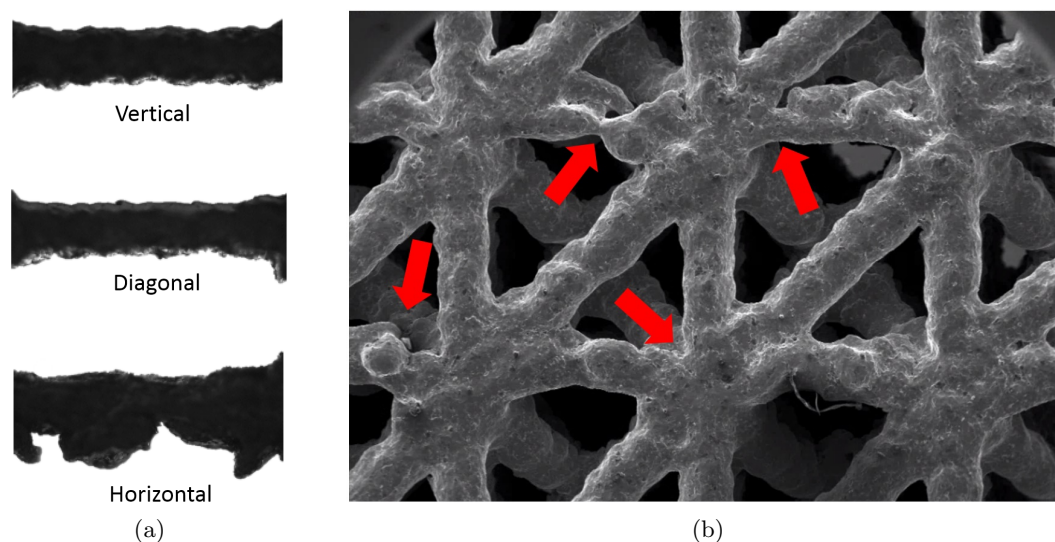
Figure 1.9: Surface morphology: a) microscopic images of single struts with different build directions showing a wave-like topological feature [19] and b) SEM image of individual struts and nodes within a lattice specimen showing irregularities, waviness and structurally related notches [17].

Compared to the roughness, the waviness, as shown in figure 1.9a, creates rather macroscopic notches that act as stress raisers on the surface. In addition, the waviness depends on the build orientation. Especially, horizontally printed struts suffer from overhanging bulges.

The same waviness is also found in lattice structures. Furthermore, the lattices suffer from abrupt irregularities as highlighted in figure 1.9b. Especially, lattices consist of trusses that are interconnected with each other at nodes. These nodes provide structurally related notches and lead to stress concentrations at the nodes, negatively affecting the fatigue performance.

In summary, the poor surface condition of lattice structures can be attributed to:

- Structurally related notches inducing stress concentrations at nodes.

- Waviness creating rather macroscopic notches.

- Microlevel roughness and surface defects acting as crack nucleation sites.

All these surface characteristics act as stress raisers on the surface and promote stress concentrations. Thus the poor surface quality in combination with the porous defects give an explanation for the inferior fatigue response of raw lattice structures summarized in table 1.1. In particular compared to solid parts, the surface of porous structures can not be machined and other post-processing treatments are necessary to improve the surface condition.

Fürer [17] applied a chemical etching to the specimens with the aim to improve the surface condition, yielding the etched lattice group. Although the etching led to 25% thinner, and thus smoother struts, the fatigue performance in terms of fatigue ratio remained unchanged. A second aspect was followed with the intention to investigate the fatigue performance of the lattices in a condition of progressed bone ingrowth. This was performed by filling the lattices with an epoxy resin yielding the epoxy-reinforced lattice group. As shown in table 1.1 the epoxy helped to improve the fatigue ratio.

1.5. Objectives

As explained above, the lattices suffer from a poor surface quality and internal defects reducing the fatigue life. With respect to residual stresses and microstructure, there is only little room for improvement, as the lattices already underwent post-process heat treatment. However, a promising and reasonable aspect in improving fatigue strength is reducing stress concentrations. As shown above, there are multiple potential stress raisers acting on the lattice structures. Thus, the objective of this work is to investigate the effect of surface modifications on the fatigue performance of a series of SLM Ti-6Al-4V miniature tensile specimens. These specimens represent single struts of the lattice and allow to demonstrate the effect of surface modifications in an isolated manner, before being applied to lattices. Furthermore, the application of the different surface modifications on lattice structures is investigated and assessed within this work in terms of feasibility. One important aspect of this involves the homogeneity of the surface modification process within the whole structure which should be provided in order to cover all the surface, and thus, all potential surface defects.

1.5.1. Chemical etching

Although, the effect of surface roughness on the fatigue life was explained above, a clear explanation for the unchanged fatigue ratio using etched lattices is still missing. Therefore, it makes sense to further investigate the effectiveness of chemical etching by examining the effect on single miniature tensile specimens.

For the chemical etching of Ti-6Al-4V, Kroll's reagent etchant containing nitric acid (HNO_3) and hydrofluoric acid (HF) is used as it offers a relatively fast pickling rate for efficient material removal. However, a fast pickling rate goes in hand with a higher final surface roughness [39]. Thus to induce surface smoothing, a milder etchant mixture below 1% HF should be considered.

Furthermore, Dong et al. [40] reported that the surface finish improves with increasing material removal. Therefore, a geometric compensation strategy makes sense in order to prevent size effects between different sample groups, and in particular, to maximize the final surface finish.

1.5.2. Coating

The outcome of the epoxy-reinforced lattices led to the following conclusion; either the epoxy prevents the bending of diagonal struts improving the fatigue response. Or, the epoxy reinforcement involves the filling of notches which helps reducing stress concentrations at nucleation sites. The idea of filling up notches with a supporting material inspired. However, a fully filled lattice does not allow for bone ingrowth anymore. This led to the approach of applying coatings with the main intention to improve fatigue performance.

In general, several mechanisms could explain an improvement in fatigue response by coating:

- The coating can take a substantial portion of the load and thus, the effective load on the strut is reduced.

- The coating penetrates into the root of crack nucleation sites. The additional path for stress transfer results in unloading of the notches and leads to lower stress concentrations. Thus, the coating can impede micro crack growth by reducing or preventing the opening of crack nucleation sites.

- The coating can impose compressive residual stresses on the surface of the struts. This can lower stress concentrations at crack nucleation sites and lead to impeded growth of micro cracks.

However, the first mechanism should be avoided as much as possible because it leads inevitably to a higher stiffness response of the overall structure. It is important to not further increase the stiffness of the lattice structure due to the mechano-biological requirement imposed by stress shielding effects between implant and bone. Therefore, the objective of the coating is to improve the fatigue performance while keeping the stiffness response unaffected as much as possible at the same time. Applying the rule of mixture on two concentric cylinders yields:

$$E_{overall} = v_{strut} \cdot E_{strut} + v_{coating} \cdot E_{coating} \tag{1.3}$$

where v is the volume fraction and E is the elastic modulus. In order to keep the additional term of the coating small, two approaches can be followed. On the one hand, a thick coating but with a rather small stiffness can be applied. On the other hand, a thin coating with a higher stiffness can be used. Both approaches are examined within this work.

Nowadays, various coating methods exist. However, only a few have the ability to homogeneously coat complex geometries, such as the electrophoretic deposition method, dip or spin coating, and the biomimetic dip coating approach [41]. For this work, the dip or spin coating method was chosen due to its simplicity compared to the other ones.

Addressing the thick coating approach, the use of a biocompatible polymer was taken into consideration. A lot of different biopolymers with various properties are available

for the use in biomedical applications. In order to reduce stress concentrations in the lattices, a polymer with some remarkable stiffness should be considered. Polymethyl methacrylate (PMMA) is FDA-approved, bioinert, chemically stable, durable and is widely used in the biomedical field e.g. in bone cements, denture resin, drug delivery systems, biosensors and medical devices [42]. Films of PMMA are also used for corrosion protection and optoelectronic devices [43]. Especially, the use of high molecular weight PMMA is attractive due to enhanced stiffness and mechanical strength compared to low molecular mass PMMA, which are 3 GPa and 90 MPa, respectively [44]. In addition, the requirements for dip or spin coating of the lattices necessitate the fine tuning of the coating viscosity. The ability to adapt the viscosity of the PMMA slurry, by mixing the appropriate ratio of PMMA powder to liquid monomer [44], makes PMMA an optimal candidate for the use as coating material. Ceramic nanofillers, such as titanium dioxide (TiO_2), are added to PMMA creating a hybrid organic-inorganic nanocomposite coating for enhanced corrosion protection of biomedical implants [45, 46, 47]. The addition of TiO_2 nanofillers provides an additional benefit for the coating, such as improved bioactivity, enhanced corrosion protection [46] and mechanical strength [48].

TiO_2 has received considerable attention as coating material due to its bioactive, antimicrobial and corrosion-protective properties. In fact, the excellent biocompatibility of titanium and its alloys is attributed to the formation of an oxide film containing mainly TiO_2. Thus, the TiO_2 layer plays a major role in the long-term stability of titanium-based implants [49, 50, 51]. The surface TiO_2 is essential for a better osseointegration [52, 53], which depends on the initial attachment as well as adhesion and spreading behaviour of the surrounding cells at the bone-implant interface [54]. These events can be affected by characteristics of the implant surface, involving chemical composition, wettability and morphology [55]. The formation of a bone-like apatite layer on the implants surface is the major requirement for biomaterials to be bioactive and to bond to living bone tissue. Using simulated body fluid (SBF), this phenomenon can be reproduced in vitro; hence, the bioactivity of a biomaterial can be assessed. SBF is a solution with ion concentrations similar to those of human blood plasma [56]. Spontaneous nucleation of apatite crystals was reported to occur on the surface of TiO_2 [51].

In the recent years, the fabrication of nanostructured materials has gained a lot of interest due to their outstanding properties [57]. Nanocrystalline bioceramics can be synthesized via alkoxy-derived route. The so-called sol-gel process inherently produces ceramics with a similar grain size and microarchitecture as that of native bone [58]. Compared to conventional formulations of the same material, nanophase materials are characterized by a higher surface area and surface reactivity leading to a desirable cellular response and ultimately resulting in high osseointegration [59]. In addition, the discovery of ductility and superplasticity in nanostructured ceramics and oxides has opened up the opportunity for load-bearing coating applications [60]. Ibrahim et al. [61] were able to significantly increase the fatigue strength of steel specimens by coating with nanophase TiO_2 in comparison to coating based on conventional TiO_2, both deposited using thermal spraying. The improvement was attributed to the enhanced stiffness, imparted

compressive residual stresses, and to the higher crack propagation resistance associated with nanostructured TiO_2 [61]. Shirkhanzadeh et al. [62] reported that alkoxy-derived anatase TiO_2 coatings may exhibit superplasticity at room temperature and that they attract calcium and phosphate ions from physiological environments inducing the nucleation of an apatite layer, thus showing bioactivity [63]. Furthermore, nanostructured TiO_2 coatings deposited via sol-gel method on titanium substrates were reported to have outstanding mechanical properties such as high bonding strength and elastic modulus, specifically 70 MPa [64] and 70 GPa [65], respectively. The outstanding properties of nanocrystalline TiO_2 makes it an optimal and promising candidate for the thin coating approach addressed within this work.

To summarize, the objective of this work is to show the effectiveness of surface modifications on the fatigue response of SLM Ti-6Al-4V miniature tensile specimens representing individual struts of the lattice structure. In particular, the surface modifications involve a chemical etching with Kroll's reagent, a thick, biocompatible PMMA based coating and a thin, bioactive nanophase TiO_2 coating. Furthermore, the application of the mentioned surface modifications on lattices is investigated with respect to feasibility.

2. Materials and methods

In this chapter, the sample preparation involving the sample fabrication, chemical etching, coating fabrication and coating deposition as well as the test setup are described.

2.1. Material

The effectiveness of different surface techniques on the fatigue strength is supposed to be demonstrated and understood using miniature tensile specimens before applying it on the lattices. These specimens represent the struts which the lattice structure is comprised of; thus, these test specimens are further simply referred to as struts. The struts were previously manufactured by the British company Renishaw using an AM250 system at 200W. The axis of building direction was aligned with the longitudinal axis of the strut, the layer thickness was 30 μm and a post-process annealing at 850°C for two hours was performed. In particular, neither a surface treatment nor HIP was applied. The struts used for this investigation have a nominal diameter of 200 μm, except for the etched sample group which started with a nominal diameter of 300 μm.

2.2. Chemical etching

Pursuing a geometric compensation strategy, the chemical etching was performed on struts with a nominal diameter of 300 μm. An appropriate etching duration was followed aiming for an ultimate thickness similar to the other sample groups, i.e. struts with a nominal diameter of 200 μm; thus, avoiding size effects while maximizing smoothing effect.

The specimens were put in an etching bath for a duration of 200 minutes containing Kroll's reagent with the following concentration; 400ml H_2O + 12ml HNO_3 + 3ml HF. As described above; in order to obtain a low surface roughness, a mild HF concentration below 1% HF was used. The initial thickness of the struts was reduced by approximately 25%. The improvement in surface smoothness after chemical etching can be seen in figure 2.1.

(a)   (b)
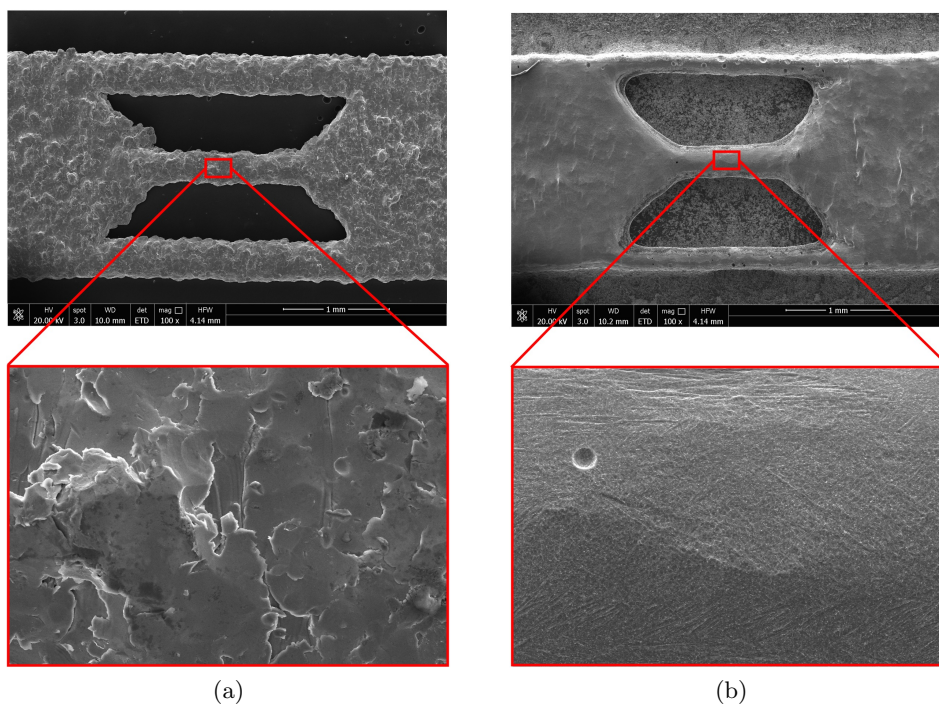
Figure 2.1: SEM images of a) a raw strut with a nominal diameter of 200μm and b) a strut after chemical etching.

2.3. Coating fabrication

2.3.1. PMMA coating

The fabrication of the PMMA coating is performed via solution blending. All reagents were purchased from Sigma-Aldrich; high molecular weight polymethyl methacrylate (HMW PMMA) with an averaged molecular mass of 350'000 g/mol, methyl methacrylate (MMA), 2-hydroxyethyl methacrylate (HEMA), benzoyl peroxide (BPO) and titanium (IV) isopropoxide. The PMMA coating is based on dip coating from a PMMA solution, i.e. PMMA dissolved in an organic solvent, and its fabrication method was adapted from [45, 46, 66]. Figure 2.2 schematically illustrates the fabrication of the PMMA coating.
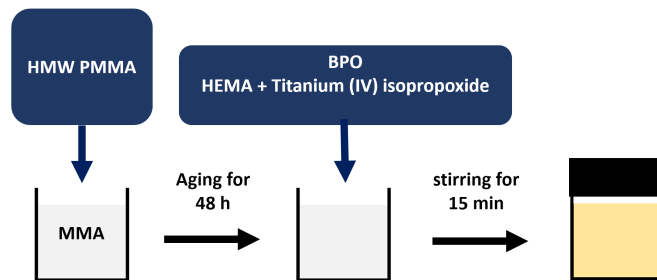
Figure 2.2: Generic illustration of the PMMA solution preparation.

2.25 g of HMW PMMA particles are mixed with 20 ml of liquid MMA, where MMA acts as organic solvent. A subsequent aging for 48 hours of the solution blend is required for the HMW PMMA particles to be dissolved completely in the solvent. 0.6 ml of titanium (IV) isopropoxide is mixed and mechanically stirred for 15 minutes beforehand together with 0.1 ml of HEMA and 0.01 ml of distilled water. At this stage, the sol-gel reactions, namely hydrolysis and condensation, start to form colloidal TiO_2 nanoparticles. Known as coupling agents, HEMA molecules have the ability to covalently bond to both TiO_2 as well as to MMA monomers. Both, the HEMA-TiO_2 mixture and 0.05 g of BPO are added to the solution blend. BPO acts as thermal activator of the polymerization process during heating. After mixture, the inorganic particles exhibited low agglomeration, yielding a well-dispersed and stable suspension that turned yellow. Additional stirring for 15 minutes completed the fabrication of the PMMA coating.

2.3.2. TiO$_2$ coating

The fabrication of the TiO$_2$ coating was performed via sol-gel approach [67] and was adapted from Kim et al. [68, 64]. In this sol-gel process, metal alkoxides are involved in hydrolysis and condensation reactions, forming a colloidal suspension, the so called 'sol'. All reagents were purchased from Sigma-Aldrich; titanium (IV) isopropoxide, 2-propanol and diethanolamine. Titanium (IV) isopropoxide is a metal alkoxide and a molecular precursor for TiO$_2$. 2-Propanol serves as solvent, diethanolamine is a gelating agent that acts as stabilizer for the sol and distilled water is necessary for the hydrolysis of the alkoxide precursor. Figure 2.3 schematically illustrates the fabrication of the TiO$_2$ coating.
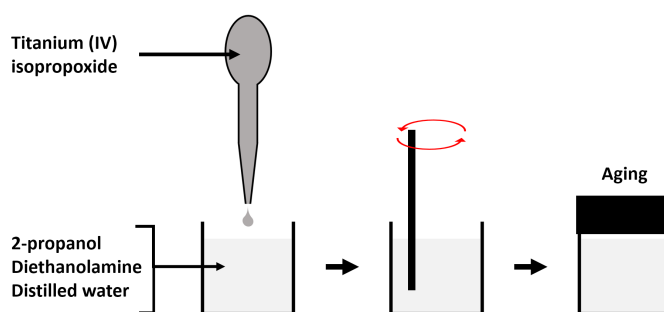
Figure 2.3: Generic illustration of the TiO$_2$ sol preparation.

To produce a stable TiO$_2$ sol, 0.5 $_M$ titanium (IV) isopropoxide was hydrolyzed dropwise in a mixture consisting of 2-propanol, distilled water and diethanolamine. The molar ratios of diethanolamine to titanium (IV) isopropoxide and distilled water to titanium (IV) isopropoxide were 1 and 2, respectively. After hydrolysis, alcohol- and water condensation starts as the hydrolyzed alkoxide molecule reacts with other alkoxide molecules. Inducing the formation of colloidal particles, hydrolysis and condensation reactions of the alkoxide group ultimately yield a well dispersed suspension of TiO$_2$ nanoparticles within the appropriate solvent. The resulting sol was mechanically stirred for 15 minutes and subsequently aged for 24 hours in a hermetically closed glass bottle to avoid contact with atmospheric water vapour. After aging, the TiO$_2$ coating fabrication is completed.

2.4. Coating deposition

The coating deposition on the struts was performed by the dip coating method, e.g. simply dipping the struts into the coating solution, treated with a subsequent drying at room temperature and heated at various temperatures. The dipping was performed with a self-designed dip coater prototype. In general, the ultimate coating thickness depends on the viscosity, withdrawal velocity and densification upon heat treatment. The dip coating method is illustrated in figure 2.4.
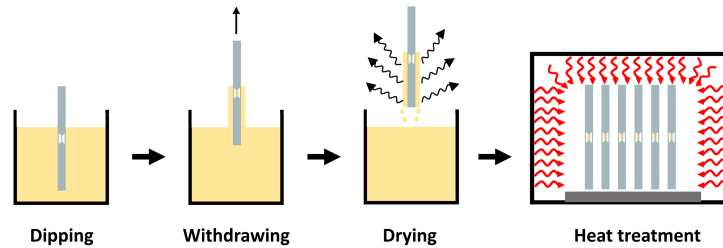
Figure 2.4: Generic illustration of the dip coating method.

2.4.1. PMMA coating

The deposition of the PMMA coating was applied as follows; after cleaning with acetone, the specimens were first moistened with liquid MMA monomer to promote better penetration of the coating solution into the root of notches. Dipping and withdrawing were performed at velocities of 0.017 mm/s and 15 mm/s, respectively. The slow dipping rate is supposed to avoid entrapment of atmospheric gas within notches. The specimens were dried for 1 hour, which is important to reduce formation of gas bubbles within the coating due to fast evaporation of the solvent. Heat treatments were performed at 60°C for 4 hours initiating heat polymerization of remaining MMA monomers within the coating. This is followed by a heat treatment at 130°C for 2 hours finishing the polymerization process. Both heat treatments were performed in an air furnace and a slow cool down was applied consecutively to avoid pre-service cracking of the film.

2.4.2. TiO$_2$ coating

The deposition of the TiO$_2$ film was applied as follows; a cleaning of the strut specimens was performed with acetone before coating. For depositing a TiO$_2$ layer, the struts were dipped into the TiO$_2$ sol with a dipping rate of 0.017 mm/s and withdrawn with a rate of 0.017 mm/s. Again, the slow dipping rate is supposed to avoid entrapment of atmospheric gas. However, high capillary activity jacked up the sol above the sol-gas border, most probably yielding a pre-moistening of the structure. As ceramic coatings via sol-gel method are prone to cracking, the applied withdrawal speed was evaluated beforehand. In general, the cracking of the film is attributed to the initial coating thickness. During heat treatment, the thermal activation provides the driving force for

the densification of the porous colloidal TiO_2 grid. As a consequence, cracking of the film can occur due to excessive transversal densification above a critical initial film thickness. Figure 2.5 shows the TiO_2 coating of glass cylinders with different withdrawal velocities. A similar critical withdrawal velocity was found for the deposition of a crack-free TiO_2 film as reported in literature [69]. Increasing of the withdrawal velocity leads to cracked TiO_2 coatings.

v=0.1mm/s

v=0.3mm/s

v=1mm/s

500 µm
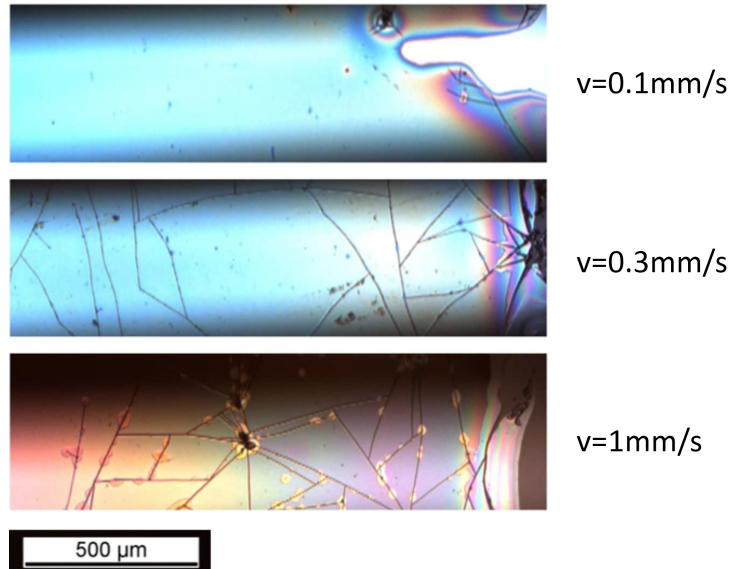
Figure 2.5: TiO_2 coating with different withdrawal velocities.

However, fabricating a crack-free TiO_2 on the struts turned out to be more challenging. The same critical withdrawal velocity leading to crack-free films on perfectly cylindric glass substrates yielded a highly cracked coating on the TiO_2 struts. As shown in figure 2.6, the coating morphology is rather a discrete coating consisting of multiple plates instead of a continuous film. The TiO_2 can be identified as small dark plates distributed over the strut, whereas the yellow area corresponds to oxidized Ti-6Al-4V.
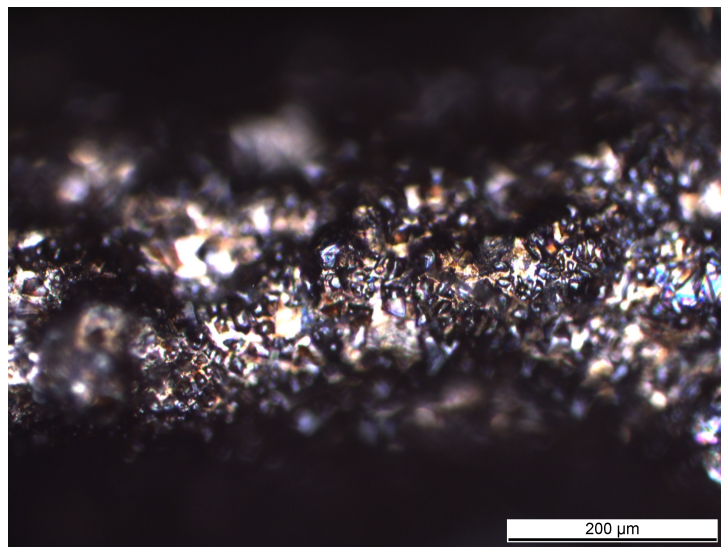
Figure 2.6: Light microscopy imaging: TiO_2 coating on a strut specimen using a withdrawal velocity of 0.1 mm/s. TiO_2 coating consists of black plates distributed over the Ti-6Al-4V strut.

The different outcomes in cracking of the coating may be induced by capillary activities on the notched and rough struts, leading to an undesirable high initial coating thickness that inevitably ends up in cracking upon densification.

Thus, the lowest possible withdrawal rate was applied, namely 0.017 mm/s in order to avoid cracking as much as possible. Drying at room temperature was applied for 1 hour and allowed the solvent to evaporate. The specimens were exposed to subsequent heat treatments, first at 80°C for 2 hours in an air furnace, forcing the evaporation of the remaining solvent molecules. This was followed by a heat treatment at 400°C in a vacuum furnace, leading to the important densification of the TiO_2 coating. Heat treatments at 400°C require a vacuum furnace to avoid oxidation of the Ti-6Al-4V. The specimens were allowed to cool down slowly after each heat treatment. The as-described procedure was applied twice in order to increase the thickness of the TiO_2 coating layer.

2.5. Test setup

Both tensile as well as fatigue tests were performed on a planar biaxial test-machine (MTS Systems Corporation). In order to fix the strut specimens, custom built aluminum clamps were used. The same initial distance between the clamps was set for all strut specimens, i.e. 9 mm. Forces were measured using a load cell with a maximum force limit of 100 N. Tensile tests were performed with a displacement rate of 0.007 mm/s. The fatigue tests were applied with a rate of 10 Hz and at a load ratio of R=0.1. A DIC-camera setup (Pike, Allied Vision) in combination with a LED ring-panel allowed the measurement of the strain within the strut specimen. An internal python script was used for the analysis of the images and strain measurements. Examples of the three different surface modifications are depicted in figure 2.7.

(a)   (b)   (c)
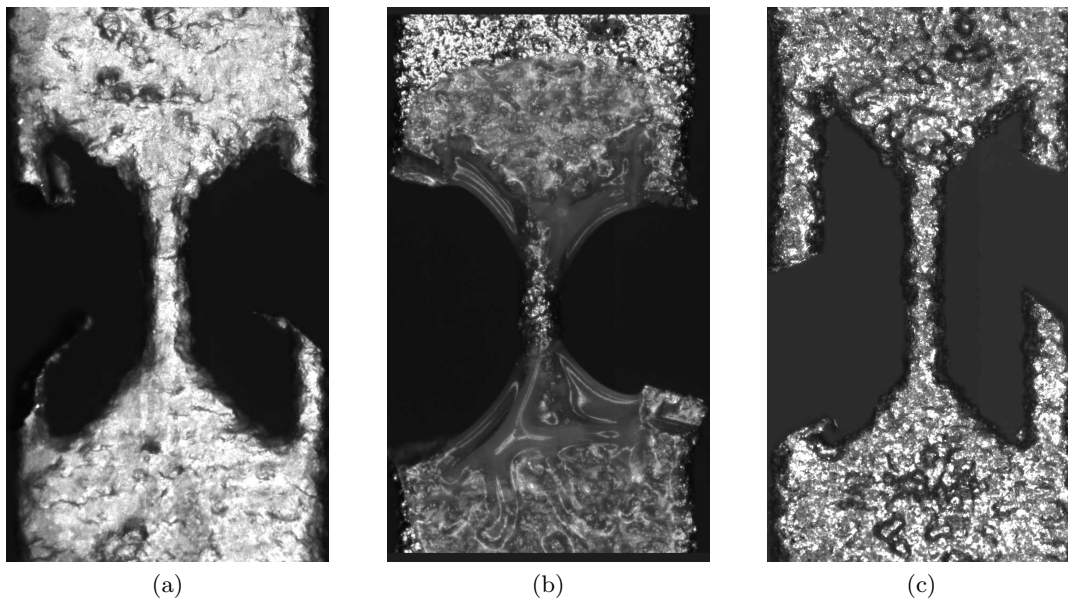
Figure 2.7: DIC images of strut specimens prepared with the corresponding surface modification: a) chemical etching b) PMMA coating and c) TiO$_2$ coating.

3. Results and discussion

In this chapter, the results of both tensile as well as fatigue tests are described. In addition, previous findings from Robmann [19] and Greenfeld [20] are considered as reference group. Furthermore, the outcome of the results are discussed with the help of additional FE models and visual observations using scanning electron microscopy (SEM) and light microscopy imaging. Furthermore, feasibility tests of the appropriate surface modifications on the lattice structures were performed and are discussed.

3.1. Experimental results

The assessment of the strut thickness was performed by light microscopy imaging, allowing to calculate the crosssectional area by assuming a round profile. Figure 3.1a shows the stress-strain response of the surface-modified struts. For each sample group, two struts were used. In order to compare the effect of surface modifications on the tensile response, previously performed tensile tests by Robmann [19] using raw struts are plotted in figure 3.1b.
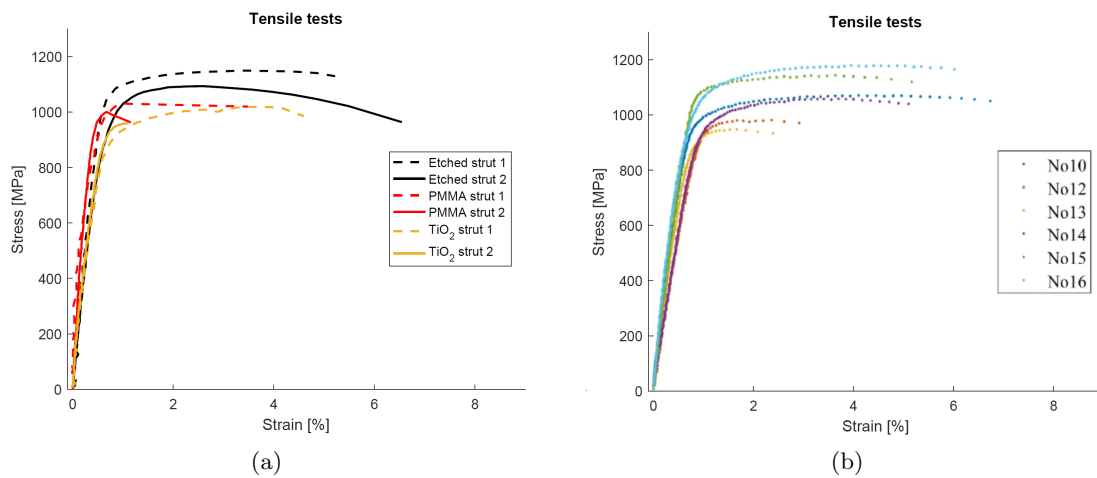
Figure 3.1: Stress-strain response of a) surface-modified struts b) raw struts [19].

The ultimate tensile strength of surface-modified struts lays within the same range as shown by Robmann [19] using raw struts. However, the elongation at break for some coated struts is lower. Calculating reasonable stiffness values turned out to be difficult due to unreliable tracking of single points on the surface of the struts, in particular on the PMMA-coated struts.

The fatigue performance of surface-modified struts is plotted in figures 3.2 - 3.4. In order to enable a comparison, the fatigue results previously measured by Greenfeld [20] using raw struts are added to the plots. Furthermore, the fatigue response at a load ratio of R=0.1 of wrought Ti-6Al-4V [25] and bulk SLM Ti-6Al-4V [38], both with machined surfaces, are added to the plots.
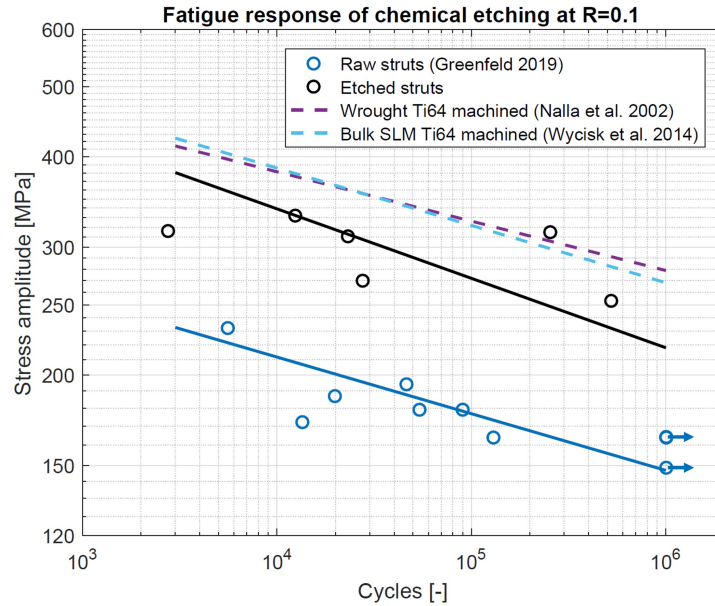
Figure 3.2: Fatigue response at R=0.1 using chemically etched SLM Ti-6Al-4V struts.

Figure 3.2 indicates that the fatigue strength at 10^6 cycles is increased by 47.7% after chemical etching. Thus, this surface modification showed to be highly effective on the fatigue performance. In spite of the smooth surface and reduced surface defects, the etched struts still do not reach the same fatigue response as wrought Ti-6Al-4V or bulk SLM Ti-6Al-4V. The discrepancy can be attributed to the presence of internal defects.
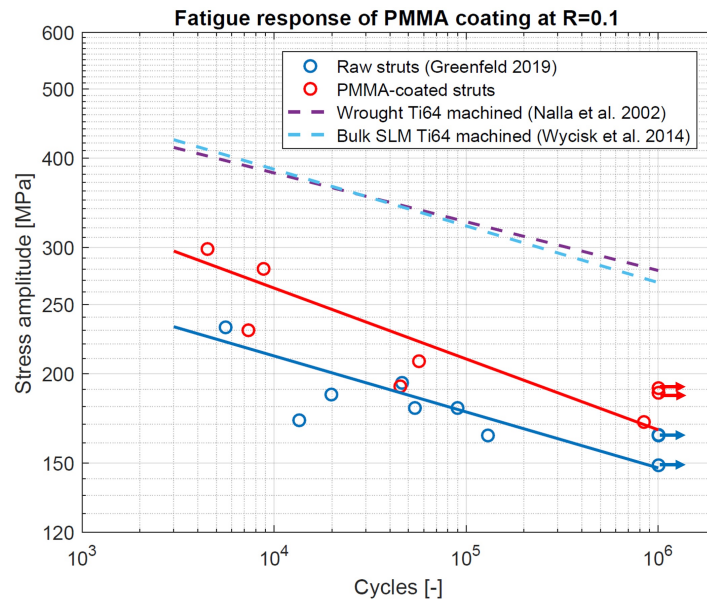
Figure 3.3: Fatigue response at R=0.1 using PMMA-coated SLM Ti-6Al-4V struts.

Figure 3.3 indicates that PMMA-coating increases the fatigue strength of struts at 10^6 cycles by 13%. Compared to raw struts, the PMMA coating shows some improvement. However in relation to wrought Ti-6Al-4V, the PMMA coating is not highly effective. The results are further explained in section 3.2.
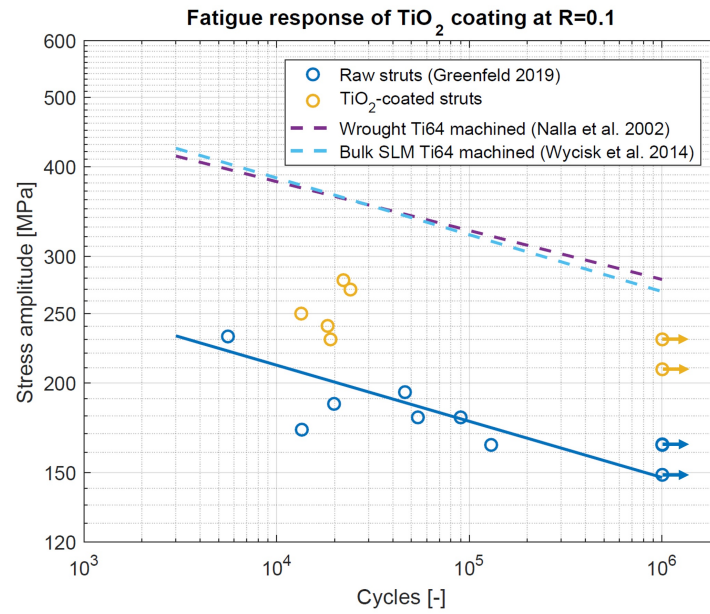
Figure 3.4: Fatigue response at R=0.1 using TiO$_2$-coated SLM Ti-6Al-4V struts.

Figure 3.4 shows; upon TiO$_2$ coating, the fatigue performance of the struts is clearly improved. Compared to the raw struts, the TiO$_2$ coating has a remarkable effect on the fatigue performance. Furthermore, the TiO$_2$-coated struts showed superior fatigue properties compared to PMMA-coated struts. However, an increased scatter can be noticed with regard to TiO$_2$-coated struts.

Comparing the fatigue results of all surface modifications with each other yields; the effect of PMMA coating on the fatigue response turned out to be least effective among the as-performed surface modifications. The improvement in fatigue performance using TiO$_2$ coating showed higher effect compared to PMMA coating. Chemical etching showed by far the best improvement in terms of fatigue properties.

3.2. Discussion

In this section, the outcome of the different surface modifications are discussed with the help of related literature, FE analysis and microscopic observations. Furthermore, an additional aspect for each surface modification, namely the feasibilty on lattice structures, is provided. The coating of lattices was performed via spin coating method, as shown in figure 3.5.

Deposition   **Spinning**   **Drying**   **Heat treatment**
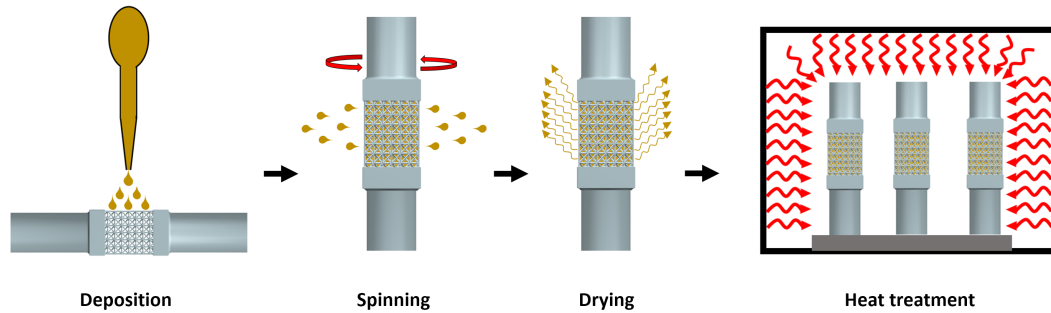
Figure 3.5: Generic illustration of the spin coating method applied on lattices.

For the FE analysis, a linear elastic model with the objective to predict the stress concentrations resulting from the macroscopic waviness of raw struts was created. Furthermore, the FE model is supposed to explain the effectiveness of a coating.

(a)   (b)   (c)
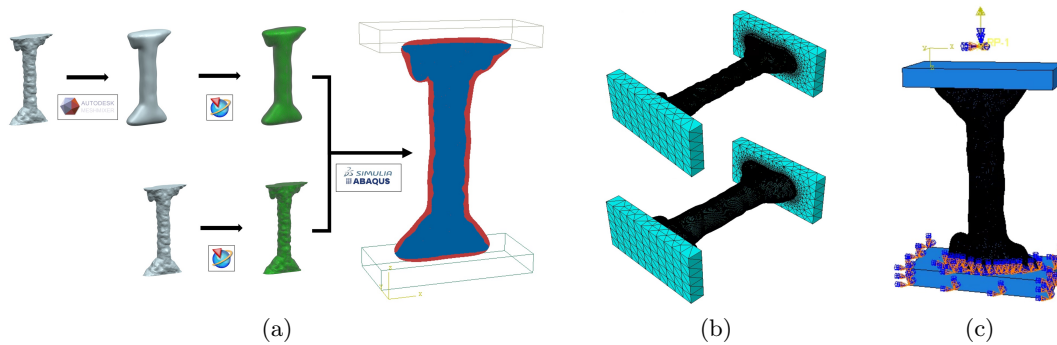
Figure 3.6: Overview of the finite element model setup; a) Coating generation and merging using μ-CT data, b) meshing using tetrahedral elements and c) application of boundary conditions and concentrated force.

Figure 3.6 shows an overview of the FE setup. Previously measured μ-CT data in form of STL-files of printed specimens were used. The STL files contain the rather macroscopic topology of the struts, which can be used to predict stress concentrations induced by those macroscopic notches. A coating was generated by the software Meshmixer. Both struts and coatings were meshed in NX and imported into ABAQUS. Merging of strut and coating geometries were performed in ABAQUS, which allowed to keep the boundary

for different material assignments, as illustrated in figure 3.6a. Material properties were assigned according to table 3.1.

Table 3.1: Material properties used for the FE model.

Part	Material property	Value
Strut	Elastic modulus	105 GPa
Strut	Poisson ratio	0.27
PMMA	Elastic modulus	3 GPa
PMMA	Poisson ratio	0.43

Both raw and coated models were created and meshed with C3D10 quadratic tetrahedron elements using a mesh element size of 0.022 mm. An appropriate load and appropriate boundary conditions were applied on the upper and lower block, respectively, as shown in figure 3.6c.

3.2.1. Chemical etching

Optical observations of the specimens reveal; there are multiple explanations for the fatigue performance improvement induced by chemical etching. In figure 3.7, SEM images show the surface of raw and etched specimens.

(a)   (b)
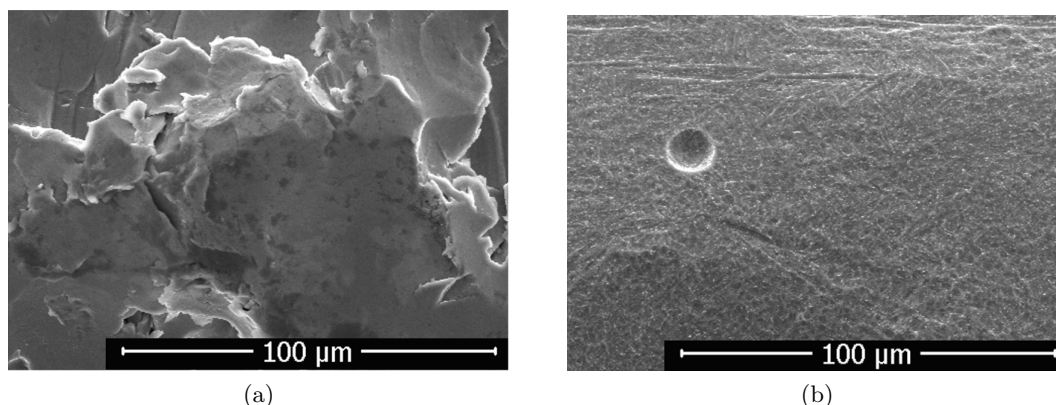
Figure 3.7: SEM imaging showing the surface roughness of the struts; a) raw strut and b) chemically etched strut.

As can be seen, chemical etching induces a highly improved surface roughness and thus, removes crack nucleation sites that act as notches on a microlevel. As a consequence, stress concentrations acting on the surface are reduced and lead to an improved fatigue response. In addition to the microscale benefits of etching, the prolonged etching duration in combination with a geometric compensation strategy allows to remove a

substantial part of the material. Thus, this leads not only to an improved microscopic roughness but also it leads to the removal of surface defects and highly decreases the macroscopic waviness. Figure 3.8 highlights the topological waviness of both struts and shows an additional, rather macroscopic smoothing effect when comparing each other.

(a)   (b)
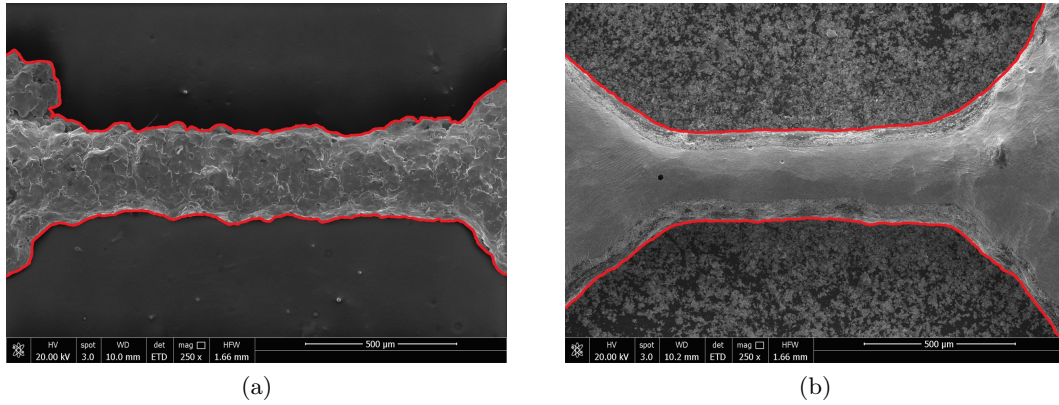
Figure 3.8: SEM imaging showing the highlighted macroscopic topology of the struts: a) raw strut and b) chemically etched strut.

The waviness creates macroscopic notches that induce stress concentrations on the surface. Using the FE model of a raw specimen, these stress concentrations can be predicted, as shown in figure 3.9. Appropriate stress concentration factors K_t are summarized in table 3.2.
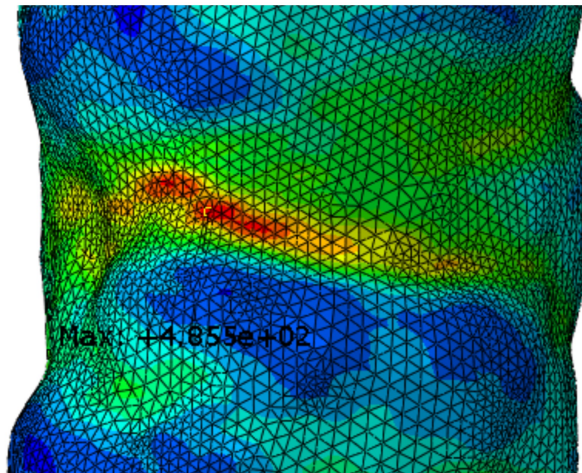
Figure 3.9: FE model of a raw strut showing stress concentrations at a critical macroscopic notch.

Table 3.2: FE predictions using a raw strut; stress concentrations arising from macroscopic notches.

Reference stress	Nominal stress [MPa]	Maximum stress [MPa]	K_t factor [-]
Mises stress	163	485.5	2.98
Maximum principal stress	163	537.9	3.3

The FE predictions suggest that stress concentrations imposed by macroscopic notches are quite high. Thus, a substantial effect in improving fatigue performance upon chemical etching may be attributed to the removal of macroscopic notches.
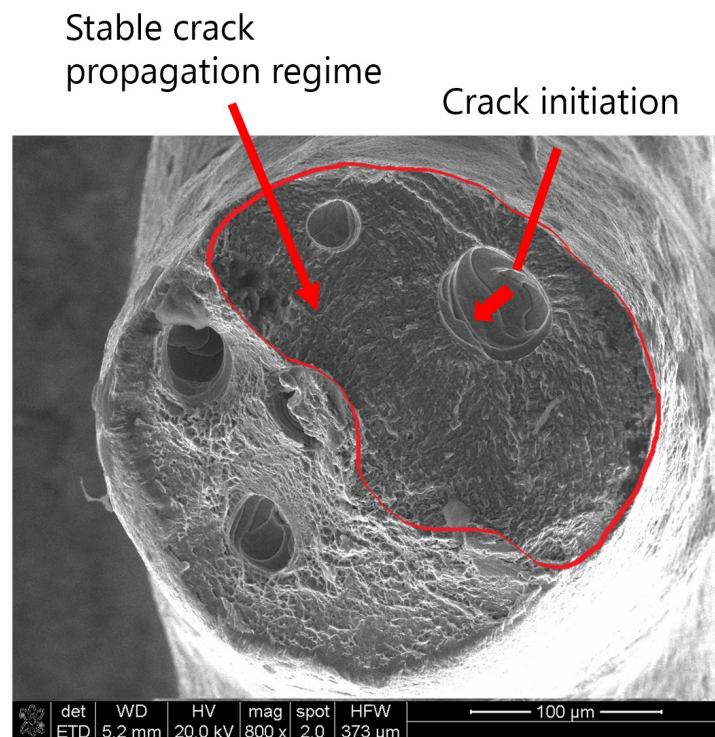
Figure 3.10: SEM observation of the fracture surface of a chemically etched strut showing; the crack initiated from an internal defect.

Furthermore looking at figure 3.10, the fracture surface of chemically etched struts reveals that the surface quality is considerably improved. With regard to chemically etched struts, the surface is no more the detrimental feature that leads to a restricted fatigue performance of the strut. Instead, the presence of internal defects now plays a major role and is the reason for not reaching a similar fatigue performance as the one of wrought

of Ti-6Al-4V specimens. Without a doubt, chemical etching has shown to be a highly effective surface modification. However, these modifications should also be applicable to structures with a higher geometric complexity. Thus, the feasibility on lattices was tested and should be taken into account.

Provided by the swiss company 3D PRECISION SA, lattices with a tetrahedron-based unit cell were used, following a geometric compensation strategy for the etching according to table 3.3.

Table 3.3: Geometric compensation strategy followed for chemical etching on lattices.

Characteristic	Initial value	Goal
Nominal strut length	1.785 mm	1.785 mm
Nominal strut diameter	400 μm	300 μm
Nominal lattice porosity	60%	75%

Lattice structures were immersed vertically into an etching bath using the same etchant. The etching was performed under magnetic stirring and for a duration of 4.5 hours until the visible struts were reduced to the targeted thickness. The lattices were cut to enable the assessment of both inner and outer struts. Accordingly, SEM images are provided in figure 3.11
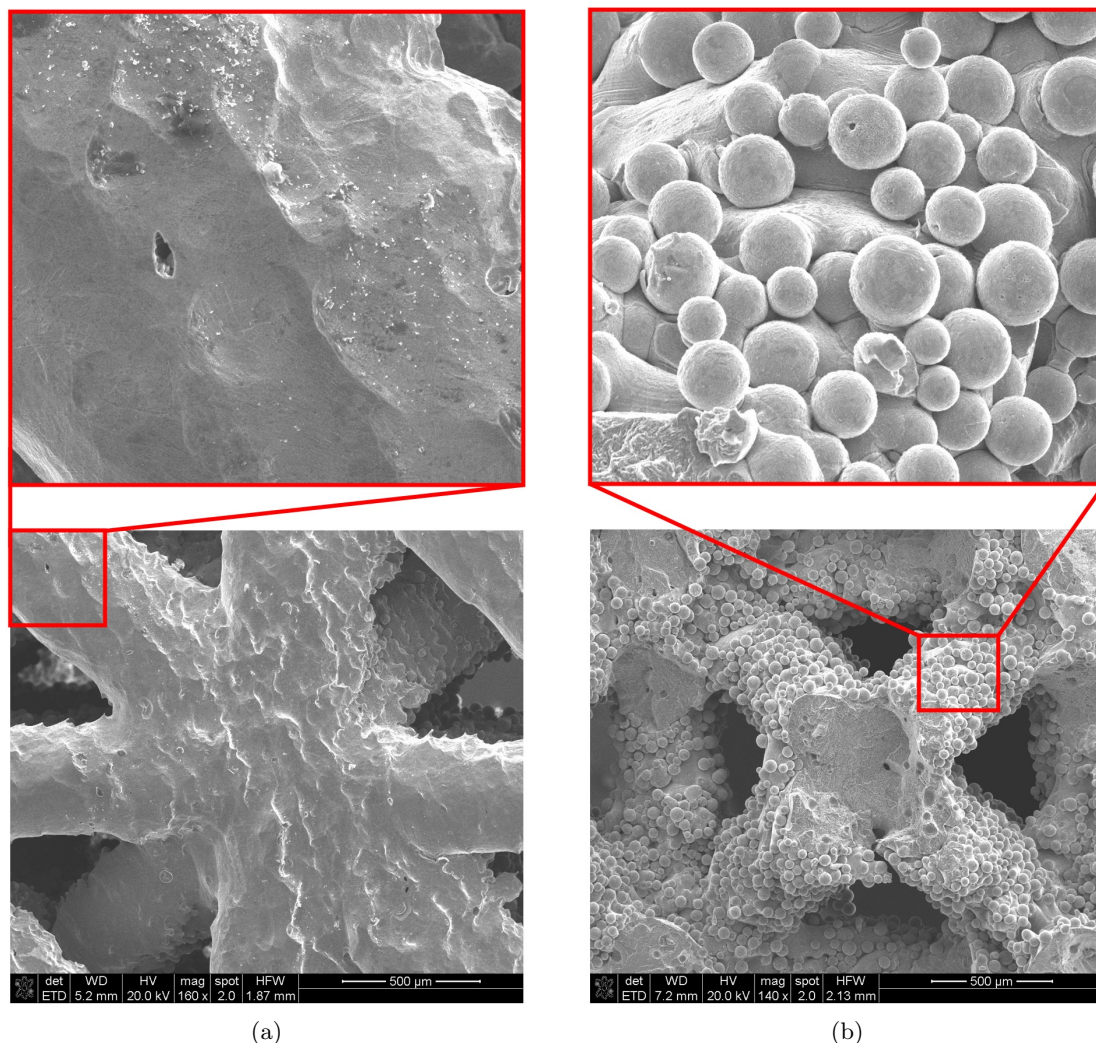
Figure 3.11: SEM imaging of nodes at different locations within etched lattice: a) outer node and b) inner node.

Figure 3.11a reveals; outer struts show reduced surface roughness and a reduced waviness, at least for the vertically printed struts. However, the diagonally and horizontally printed struts have a potential for improvement in terms of removing stair-step notches.

In comparison, figure 3.11b shows; chemical etching is less effective in internal structures. First of all, partially melted particles are still attached to the internal parts. Looking across these particles, the surface roughness seems to be smooth. However, the waviness could not be removed. This shows that the desired material removal could not take place and can be explained by two mechanisms. Either the diffusion rate within the lattices is limited, creating inhomogeneous, and especially, not persistent etchant concentrations within internal parts. Or upon etching reaction, gas bubbles are formed

and entrapped within the vertically oriented lattices, and thus, impeding mass transfer and causing inhomogeneous exposure to the etchant. It should be noted, that not even the imposition of a flux within the etching bath could avoid the inhomogeneous outcome of the etching.

In order to use the powerful benefits of chemical etching, the necessary mass transfer must be induced to obtain homogeneous results. The as-performed chemical etching does not fulfil the homogeneity requirement for lattices. In addition, the outcome of the feasibility tryouts may provide an explanation for the previous results from Fürer [17] when using etched lattices. As reported by Fürer [17], the thickness of the outer struts was reduced by 25% but simultaneously, the apparent stiffness only decreased by 9.2%. This indicates non-uniform material removal upon etching and may be the cause for the previously reported ineffectiveness of chemical etching on the fatigue ratio of lattices. However, a clear conclusion can not be drawn from this. Still, the structurally related notches at the nodes can play a major role in the ineffectiveness of chemical etching on the fatigue ratio of lattices.

Certainly, the feasibility tryouts yield that the chemical etching process on lattices necessitates optimisation in order for lattice structures to take advantage of the as-shown benefits upon chemical etching. In addition, the homogeneity is required to remove particles before implantation in order to avoid detaching of particles and their distribution within the surrounding tissue.

3.2.2. PMMA coating

SEM imaging of a PMMA-coated strut shows how macroscopic notches are filled with PMMA, as can be seen in figure 3.12.
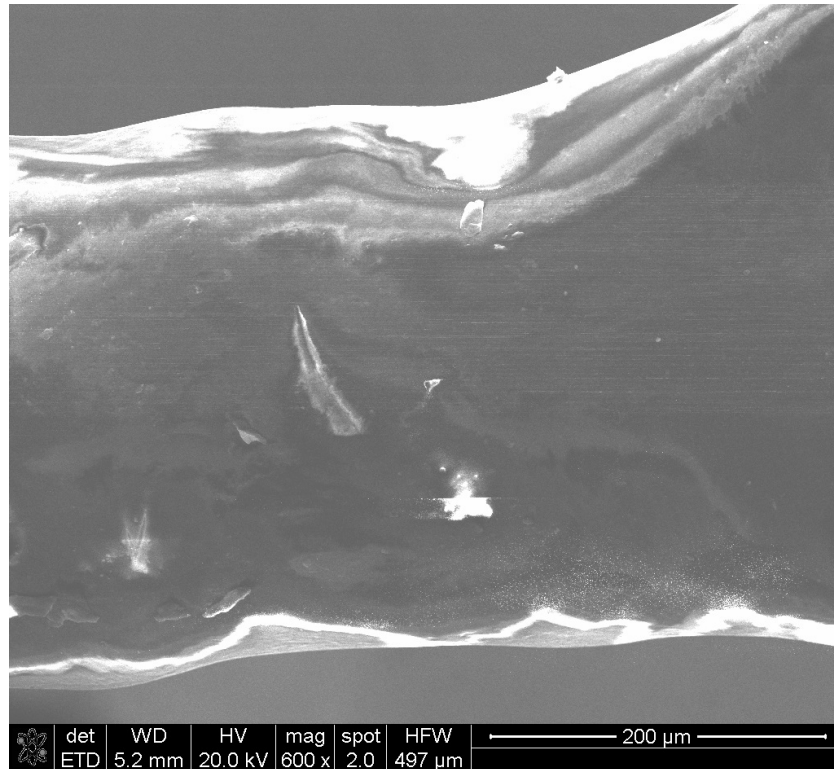
Figure 3.12: SEM image showing macroscopic notches filled with PMMA.

In order to further understand the mechanism behind the PMMA coating, FE models of coated struts are used to demonstrate the mechanical interaction between coating and strut. Figure 3.13 shows the effect of coating thickness on the reduction of stress concentrations acting at the most critical macroscopic notch.
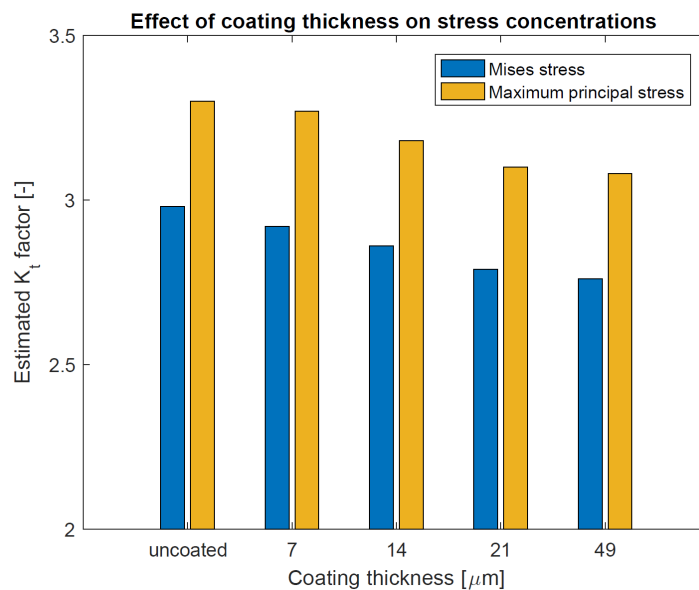
Figure 3.13: FE prediction showing the effect of coating thickness on the stress concentration factor K_t.
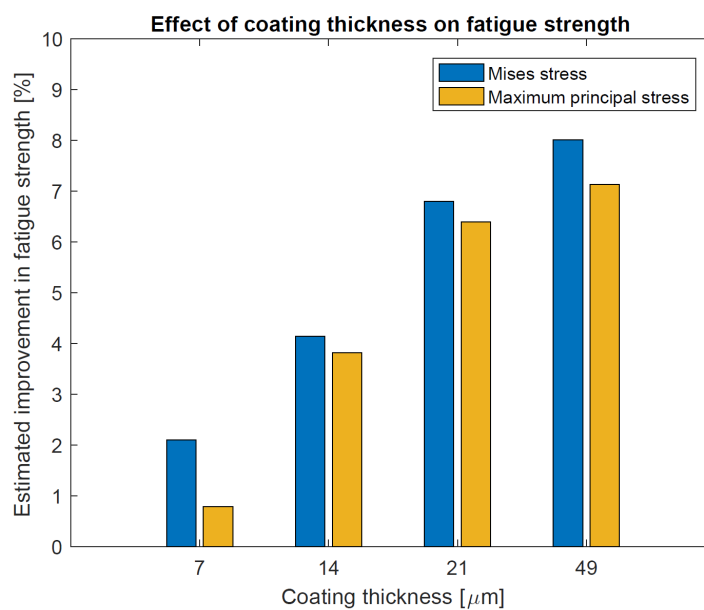
Figure 3.14: FE prediction showing the effect of coating thickness on improvement in fatigue strength.

The FE results depicted in figure 3.13 show; the PMMA caoting acts within macroscopic notches and reduces stress concentrations. Figure 3.14 illustrates the estimated

improvement in fatigue strength upon reduction in stress concentrations. These predications match the results obtained from experimental testing and indicate that the effect of PMMA coating on the fatigue improvement of struts is based on reducing stress concentrations within macroscopic notches. However, the improvement in fatigue response is only marginal. PMMA tensile specimens according to ASTM D1708-18 were fabricated with the appropriate PMMA coating material and tensile tests were performed, yielding a stiffness of 2.48 GPa. The inferior improvement in fatigue response of the PMMA-coated struts is attributed to the relatively low stiffness of the PMMA coating.

Moreover, the feasibility of homogeneously coating lattices with the as-fabricated PMMA solution turns out to be highly challenging.

| (a) | (b) |
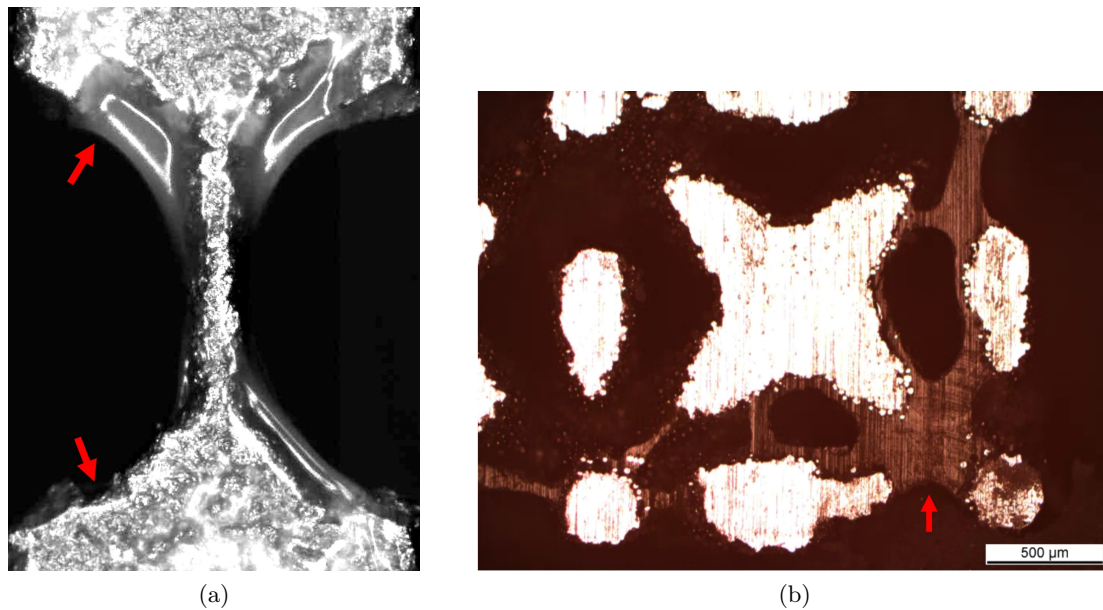
Figure 3.15: Optical observations showing the highlighted PMMA coating on: a) strut and b) lattice.

The PMMA coating tends to agglomerate due to its surface energy, resulting in a poor wettability. This is even observed on the PMMA-coated strut specimens. Looking at figure 3.15a; the coating agglomerates at concavities and yields a high coating thickness, whereas flat parts are not massively coated.

This agglomeration issue is also observed within the lattice, making a homogeneous coating very challenging. When depositing the coating solution within the lattice structures, the liquid coating has to be forced out by spinning in order to overcome the capillary activity, which keeps the liquid coating within the lattice. The additional capillary activity in combination with the poor wettability makes it difficult to obtain perfectly homogeneous coatings with thicknesses between 20 and 50 μm.

Instead, the coating of the lattices is characterized by a high inhomogeneity. In partic-

ular, the PMMA coating creates inter-strut connectivities, ending up in sealing lattice
pores instead of enveloping single struts, as shown in figure 3.15b.

Therefore, the feasibility tryouts yield; the as-fabricated PMMA solution blend is not
suitable for a homogeneous coating of lattice structures via spin coating method.

3.2.3. TiO₂ coating

As shown by the experimental results, the TiO$_2$ coating performed better compared to the PMMA coating. Optical observations show that the coating is very thin and covering the whole strut, as figure 3.16a indicates. Thus, two big advantages over the PMMA coating are provided by thin coatings; they allow the selection of stiffer coating materials while minimizing changes in the stiffness of the overall structure. The higher stiffness of the coating promotes the effectiveness in fatigue improvement. Furthermore, a thin coating does not reduce the pore size of lattices, which is important to maintain bone ingrowth capabilities.
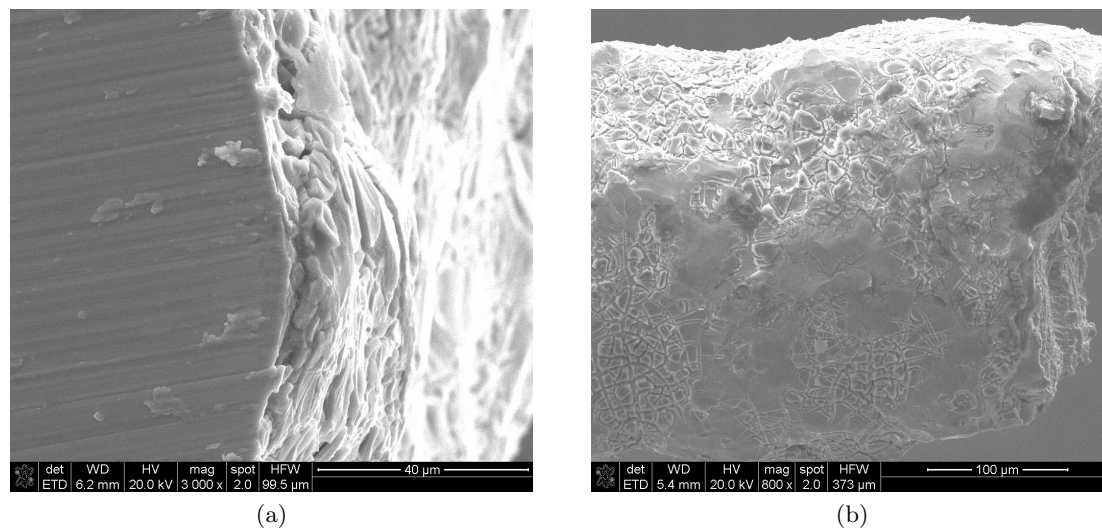
Figure 3.16: SEM imaging of TiO$_2$-coated struts at different orientations: a) longitudinal and b) transversal.

However, the coating thickness is much bigger than reported in [68, 64, 69]. As already mentioned in chapter 2, the TiO$_2$ coating suffers from cracking upon lateral densification when the initially deposited coating thickness becomes too large. In particular, the uneven and rough surface of SLM Ti-6Al-4V struts cause capillary activity, which may explain the higher thickness and inevitable cracking of the coating. Even lowering the initial thickness by decreasing the withdrawal rate could not avoid cracking of the TiO$_2$ coating, as shown in figure 3.16b. On the one hand, the coating at some locations could rather be described as discrete distribution of plates instead of a continuous film. On the other hand, there are some spots showing a crack-free TiO$_2$ film. The inhomogeneous cracking pattern also indicates, that the cracking may result from local changes in initially deposited thickness caused by capillary activities.

The presence of cracks indicates that compressive residual stresses are generated upon heat treatment on the strut specimen. The TiO_2 was shown to be capable of improving the fatigue response of the struts, which could be explained by two mechanisms:

- Compressive residual stresses are generated on the surface of the strut upon densification of the coating. Compressive residual stresses help impeding crack nucleation at crack initiation sites located on the surface.

- The TiO_2 coating penetrates into microlevel notches and prevents crack nucleation by reducing stress concentrations at the root of the notch.

In figure 3.17, the different surface qualities for raw and TiO_2-coated struts can be compared.

(a)   (b)
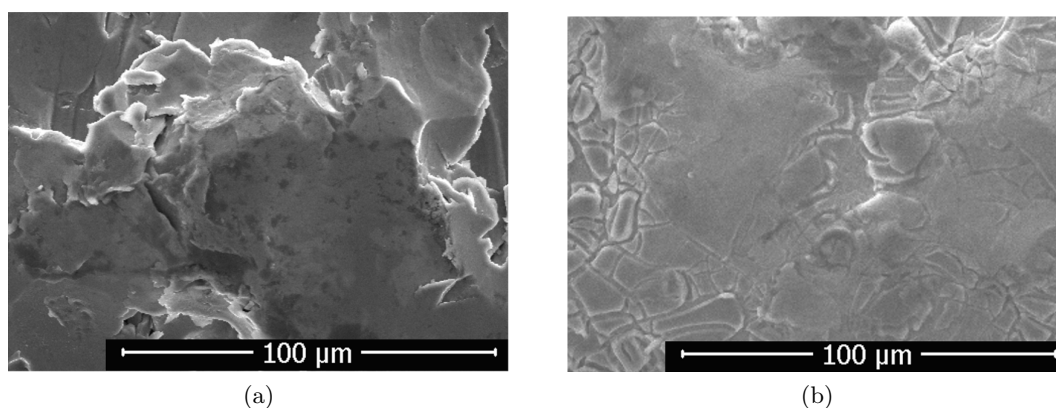
Figure 3.17: SEM imaging showing the surface roughness of the struts; a) raw strut and b) TiO_2-coated strut.

Particularly, both mechanisms are promoted by the high elastic modulus of TiO_2 and its outstanding bonding strength to Ti-6Al-4V substrates. However, the fatigue improvement, despite cracking of the TiO_2 coating, necessitates further explanation. In general, the introduction of micro cracks on the surface is expected to negatively influence the fatigue response. However, a negative effect was not measured and may be a consequence of improved ductility and fracture toughness reported for nanophase structured ceramics [70]. In particular, Shirkhanzadeh et al. [62] were able to show that nanocrystalline anatase TiO_2 coatings exhibit significant plastic deformation at room temperature.
Another explanation might be that the coating is applied on a surface that is already characterized by a poor surface condition. Nonetheless, avoiding cracking of the TiO_2 film is not only desirable in terms of fatigue improvement of the strut specimens, but also a crack-free coating ensures a persistent coating service life, providing an implant with bioactive, antimicrobial, corrosion-protective as well as improved tribological properties, and preventing the release of metallic ions into the surrounding tissue.
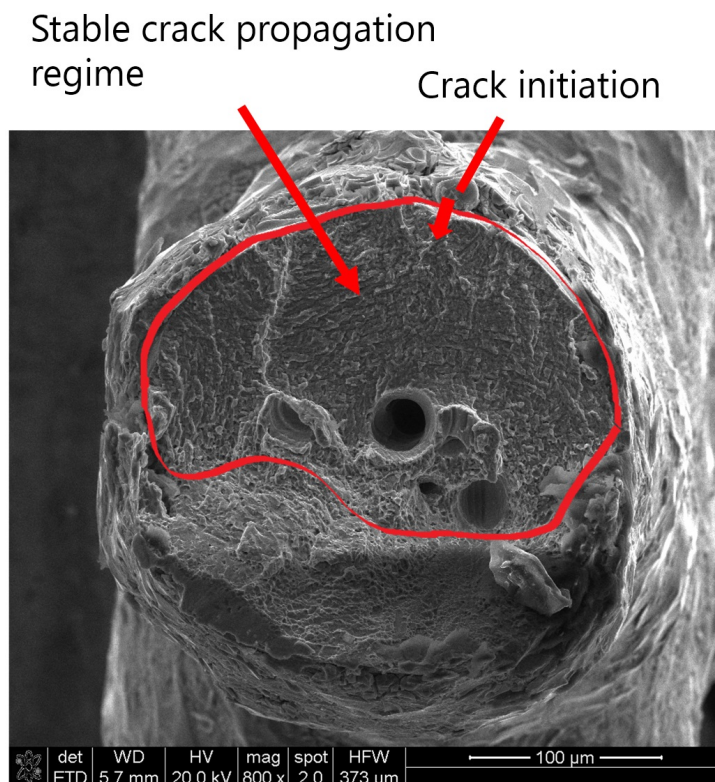
Figure 3.18: SEM observation of the fracture surface of a TiO$_2$-coated strut showing; the crack initiated from the surface.

Looking at the fracture surface of TiO$_2$-coated struts as shown in figure 3.18 reveals: the coating is not fully able to prevent crack initiation from the surface. Thus, further optimisation of the coating on SLM Ti-6Al-4V specimens is highly suggested, not only from a biocompatible perspective, but also from a mechanical one.

The feasibility tryouts performed on the lattice structures revealed; the TiO$_2$ coating is applicable on the lattices via spin coating method. In order to decrease the deposition thickness and to avoid cracks, a very high rotational speed is required. Furthermore to increase centrifugal forces, the rotational axis can be shifted. The lattices were placed on a disc 5 mm off the rotational axis and were rotated at 2700 rpm for 20 seconds. Thus, the liquid sol is forced out unidirectionally.
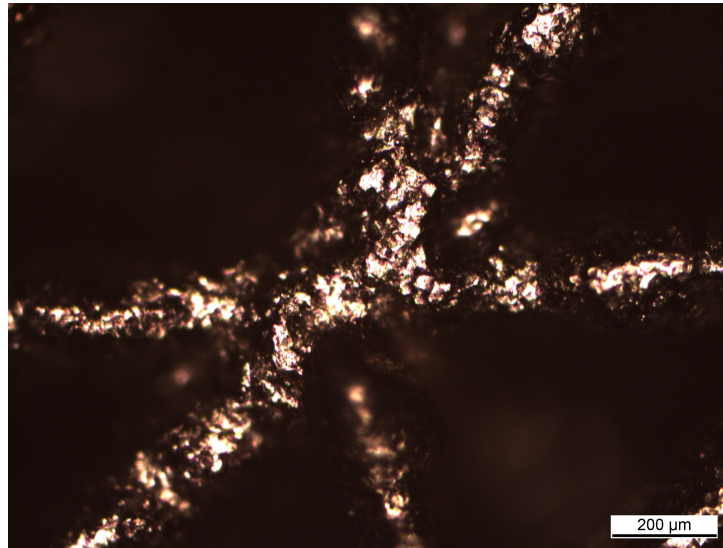
Figure 3.19: Light microscopy imaging showing the node of a TiO$_2$-coated lattice, located at the side were the sol is forced out.

Figure 3.19 shows the node located at the side were the sol is forced out. The coating reveals; a homogeneous coating deposition on lattice structures using sol-gel derived TiO$_2$ is possible via spin coating method. The coating feasibility is mainly enabled by the good wettability and low viscosity of the TiO$_2$ sol. However, the TiO$_2$ coating is still cracked, necessitating the optimisation of the coating deposition method.

Improvement in coating quality may be reached by changing to a more controlled deposition method. Coating via electrophoresis seems to be promising and is more suitable because this deposition method should not be influenced by the capillary activity. Furthermore, Shirkhanzadeh et al. [62] were able to deposit a crack-free, 40 μm thick nanophase TiO$_2$ film. The same thickness deposited with dip coating would yield a highly cracked surface upon densification [69]. Thus, the electrophoretic deposition method is promising to create crack-free TiO$_2$ coatings on SLM Ti-6Al-4V specimens.

4. Conclusions and outlook

Fatigue tests of SLM Ti-6Al-4V miniature tensile specimens, representing individual struts of lattice structures, were performed. The effect of different surface modifications, such as chemical etching, PMMA coating and TiO_2 coating were investigated. The fatigue results were interpreted with the help of microscopical observations and FE analysis. Furthermore, each surface modification was applied on lattice structures and assessed in terms of feasibility. Thus, this preliminary work provides a basis for future fatigue improvements of lattice structures used in orthopaedic applications. In summary, the conclusions drawn from this investigation are as follows.

Chemical etching:

- Chemical etching showed the best effectiveness in terms of fatigue response improvement among all surface modifications.

- The fatigue strength compared to raw struts was improved by 47.7%.

- The high effectiveness can be attributed to the removal of macroscopic notches, the removal of surface defects and to a smoother microlevel roughness, eliminating crack nucleation sites and reducing stress concentrations.

- The application of chemical etching on lattices turned out to be challenging; chemical etching is impaired within internal structures leading to ineffective removal of macroscopic notches, surface defects and partially molten particles.

- To take advantage of chemical etching for lattices, the etching process requires an imposed mass transfer within internal parts of the lattices in order to satisfy homogeneity.

PMMA coating:

- PMMA coating was least effective in terms of fatigue response improvement among all surface modifications.

- The fatigue strength compared to raw struts was improved by 13%.

- The improvement in fatigue response can be attributed to the unloading of the effective load working on the strut and to the reduction in stress concentrations at crack initiation sites. However both mechanisms are rather weak due to the relatively low stiffness of the PMMA coating.

- The application of the PMMA coating on lattices was not successful; the PMMA coating tends to agglomerate due to high surface tension, resulting in non-homogeneous coating and sealing of lattice pores.

TiO_2 coating:

- TiO_2 coating showed the better effectiveness in terms of fatigue response improvement for struts compared to PMMA coating.

- The fatigue strength compared to raw struts was considerably improved.

- The improvement in fatigue response can be attributed either to the imposition of compressive residual stresses on the surface of the strut specimens or to the reduction in stress concentrations at microlevel crack initiation sites by impeding crack nucleation.

- Despite optimisations of the coating deposition, cracking of the TiO_2 coating could not be avoided, which could be explained by non-uniform coating thickness upon capillary activity caused by uneven and rough surfaces.

- The cracking of the coating could explain the higher scatter that was obtained in the fatigue results of TiO_2-coated struts.

- The application of the TiO_2 coating on lattices via spin coating was successful due to the desirable wettability and resulted in a homogeneous coating.

The as-shown investigation revealed the effectiveness of different surface modifications using struts and assessed their feasibility on lattice structures. The as-fabricated PMMA coating was not effective enough and was not applicable on lattices. The chemical etching was highly effective but the application on lattices was not homogeneous. Thus, the optimization of the etching process could be refined by imposing a mass transfer within inner structures, eliminating inhomogeneous etching. This could be realised by using a pump system. Another possible method could take advantage of the capillary effect. Instead of staying in an etching bath, the lattices could only be dipped into the etchant. The inner structures will be filled with etchant that remains there due to capillary activity, even when being withdrawn. As soon as the entrapped etchant loses its reactivity upon saturation, the depleted etchant within the lattice can be exchanged with a fresh etchant. This process can be repeated until the desired smoothing result is reached. The big advantage over the bath method is that the outer structures will not be exposed to excessive etchant.

The TiO_2 coating showed some major advantages over the the PMMA coating. In particular, the fatigue performance was improved, the application on lattices is feasible, the coating does not compromise the lattice pore size and last but not least, TiO_2 brings superior properties such as bioactivity, antimicrobial properties, enhanced corrosion protection, high stiffness and bonding strength. However, there is still room for improvement; a crack-free TiO_2 coating could be realised by switching to another coating method. Especially, the electrophoretic deposition method could be promising concerning this matter. Furthermore, it would be interesting to investigate the combination of chemical etching and TiO_2 coating. Maybe, the smoothing effect of the chemical etching could mitigate capillary activity which causes cracking of the coating. Once a crack-free coating can be produced on SLM Ti-6Al-4V specimens, the coating could even be extended in a hybrid or bilayer fashion to a multifunctional composite coating involving additional beneficial components, such as highly bioactive hydroxyapatite, silver nanoparticles for enhanced antimicrobial properties or nanocrystalline ZrO2 for enhanced coating ductility and fracture toughness, in order to improve the long-term service life of the implant.

A. Appendix

Nomenclature

List of Abbrevations

K_t	$[-]$	Stress concentration factor
$\sigma_{nominal}$	$[MPa]$	Stress based on net cross section
σ_{max}	$[MPa]$	Peak stress at notch
E	$[GPa]$	Elastic modulus
ν	$[-]$	Poisson ratio
v	$[-]$	Volume fraction
R	$[-]$	Ratio of minimum and maximum loads during fatigue loading
N	$[-]$	Amount of cycles during fatigue testing

List of Figures

List of Tables

References

[1] M.J. Donachie. Titanium: A Technical Guide, 2nd Edition. *October*, page 128, 2000.

[2] M. I.Z. Ridzwan, Solehuddin Shuib, A. Y. Hassan, A. A. Shokri, and M. N. Mohammad Ibrahim. Problem of stress shielding and improvement to the hip implant designs: A review. *Journal of Medical Sciences*, 7(3):460–467, 2007.

[3] R. Huiskes, H. Weinans, and B. Van Rietbergen. The relationship between stress shielding and bone resorption around total hip stems and the effects of flexible materials. *Clinical Orthopaedics and Related Research*, (274):124–134, 1992.

[4] Steven Kurtz, Kevin Ong, Edmund Lau, Fionna Mowat, and Michael Halpern. Projections of primary and revision hip and knee arthroplasty in the United States from 2005 to 2030. *Journal of Bone and Joint Surgery - Series A*, 89(4):780–785, 2007.

[5] Nizar N. Mahomed, Jane A. Barrett, Jeffrey N. Katz, Charlotte B. Phillips, Elena Losina, Robert A. Lew, Edward Guadagnoli, William H. Harris, Robert Poss, and John A. Baron. Rates and outcomes of primary and revision total hip replacement in the united states medicare population. *Journal of Bone and Joint Surgery - Series A*, 85(1):27–32, 2003.

[6] Robert Pivec, Aaron J Johnson, Simon C Mears, and Michael A Mont. Hip arthroplasty. *The Lancet*, 380(9855):1768–1777, nov 2012.

[7] William D. Bugbee, William J. Culpepper, C. Anderson Engh, and Charles A. Engh. Long-term clinical consequences of stress-shielding after total hip arthroplasty without cement. *Journal of Bone and Joint Surgery - Series A*, 79(7):1007–1013, 1997.

[8] J. H. Kuiper and R. Huiskes. Mathematical optimization of elastic properties: Application to cementless hip stem design. *Journal of Biomechanical Engineering*, 119(2):166–174, 1997.

[9] Krzysztof Pałka and Rafał Pokrowiecki. Porous Titanium Implants: A Review. *Advanced Engineering Materials*, 20(5):1–18, 2018.

[10] Yingjun Wang, Sajad Arabnejad, Michael Tanzer, and Damiano Pasini. Hip implant design with three-dimensional porous architecture of optimized graded density. *Journal of Mechanical Design, Transactions of the ASME*, 140(11):1–13, 2018.

[11] Sajad Arabnejad, Burnett Johnston, Michael Tanzer, and Damiano Pasini. Fully porous 3D printed titanium femoral stem to reduce stress-shielding following total hip arthroplasty. *Journal of Orthopaedic Research*, 35(8):1774–1783, 2017.

[12] X. P. Tan, Y. J. Tan, C. S.L. Chow, S. B. Tor, and W. Y. Yeong. Metallic powder-bed based 3D printing of cellular scaffolds for orthopaedic implants: A state-of-the-art review on manufacturing, topological design, mechanical properties and biocompatibility. *Materials Science and Engineering C*, 76:1328–1343, 2017.

[13] A. J.T. Clemow, A. M. Weinstein, J. J. Klawitter, J. Koeneman, and J. Anderson. Interface mechanics of porous titanium implants. *Journal of Biomedical Materials Research*, 15(1):73–82, 1981.

[14] D. Melancon, Z. S. Bagheri, R. B. Johnston, L. Liu, M. Tanzer, and D. Pasini. Mechanical characterization of structurally porous biomaterials built via additive manufacturing: experiments, predictive models, and design maps for load-bearing bone replacement implants. *Acta Biomaterialia*, 63:350–368, 2017.

[15] William E. Frazier. Metal additive manufacturing: A review. *Journal of Materials Engineering and Performance*, 23(6):1917–1928, 2014.

[16] M Benedetti, A Plessis, R O Ritchie, M Dallago, S M J Razavi, and F Berto. Materials Science & Engineering R Architected cellular materials : A review on their mechanical properties towards fatigue-tolerant design and fabrication. *Materials Science & Engineering R*, 144:100606, 2021.

[17] Mickey Fürer. *Mechanical Behaviour of Additively Manufactured Ti-6Al-4V Lattices for Biomedical Implants*. Master thesis, ETH Zürich, 2020.

[18] Max Thalmann. *Fatigue Analysis of Selevtive Laser Melted Ti6Al4V Structures*. Bachelor thesis, ETH Zürich, 2020.

[19] Serjosha Robmann. *Deformation Analysis and Finite Element Modelling for Ti-6Al-4V Additive Manufactured Lattices*. Master thesis, ETH Zürich, 2019.

[20] Daniel Greenfeld. *Fatigue behaviour investigation of additively manufactured Ti-6Al-4V lattices*. Research report, ETH Zürich, 2019.

[21] Alexander Gillmann. *Fatigue Behavior Investigation of Additively Manufactured Ti-6Al-4V*. Research report, ETH Zürich, 2019.

[22] Daniele Ghedalia. *Characterization and modeling of orientation and size dependent tensile behaviour of AM Ti6Al4V*. Master project, ETH Zürich, 2019.

[23] A H Burstein, D T Reilly, and M Martens. Aging of bone tissue: mechanical properties. *The Journal of bone and joint surgery. American volume*, 58(1):82–86, jan 1976.

[24] Haijun Gong, Khalid Rafi, Hengfeng Gu, G. D. Janaki Ram, Thomas Starr, and Brent Stucker. Influence of defects on mechanical properties of Ti-6Al-4V components produced by selective laser melting and electron beam melting. *Materials and Design*, 86:545–554, 2015.

[25] R.K. Nalla, B.L. Boyce, J.P. Campbell, J.O. Peters, and R.O. Ritchie. Influence of Microstructure on High-Cycle Fatigue of Ti-6Al-4V: Bimodal vs. Lamellar Structures. *Metall Mater Trans A*, 33A:899–918, 2002.

[26] Jaap Schijve. *Fatigue of Structures and Materials*. Springer Science+Business Media, B.V., 2009.

[27] T. Vilaro, C. Colin, and J. D. Bartout. As-fabricated and heat-treated microstructures of the Ti-6Al-4V alloy processed by selective laser melting. *Metallurgical and Materials Transactions A: Physical Metallurgy and Materials Science*, 42(10):3190–3199, 2011.

[28] Yang Liu, Yongqiang Yang, and Di Wang. A study on the residual stress during selective laser melting (SLM) of metallic powder. *International Journal of Advanced Manufacturing Technology*, 87(1-4):647–656, 2016.

[29] Haijun Gong, Khalid Rafi, Thomas Starr, and Brent Stucker. Effect of defects on fatigue tests of as-built TI-6AL-4V parts fabricated by selective laser melting. *23rd Annual International Solid Freeform Fabrication Symposium - An Additive Manufacturing Conference, SFF 2012*, 7:499–506, 2012.

[30] Galina Kasperovich and Joachim Hausmann. Improvement of fatigue resistance and ductility of TiAl6V4 processed by selective laser melting. *Journal of Materials Processing Technology*, 220:202–214, 2015.

[31] Shunyu Liu and Yung C. Shin. Additive manufacturing of Ti6Al4V alloy: A review. *Materials and Design*, 164:107552, 2019.

[32] J Whittle, M; Levine, D; Richards. Normal gait. *Whittle's Gait Analysis*, pages 28–63, 2012.

[33] Xingchen Yan, Shuo Yin, Chaoyue Chen, Chunjie Huang, Rodolphe Bolot, Rocco Lupoi, Min Kuang, Wenyou Ma, Christian Coddet, Hanlin Liao, and Min Liu. Effect of heat treatment on the phase transformation and mechanical properties of Ti6Al4V fabricated by selective laser melting. *Journal of Alloys and Compounds*, 764:1056–1071, 2018.

[34] Novy Smokovec, Martin Frkan, Radomila Konecna, Gianni Nicoletto, and Ludvik Kunz. ScienceDirect ScienceDirect Microstructure and fatigue Ti6Al4V alloy after different stress-relief heat treatments Microstructure and fatigue performance of SLM-fabricated Ti6Al4V alloy after different stress-relief heat treatments. *Transportation Research Procedia*, 40:24–29, 2019.

[35] S Leuders, M Thöne, A Riemer, T Niendorf, T Tröster, H A Richard, and H J Maier. On the mechanical behaviour of titanium alloy TiAl6V4 manufactured by selective laser melting : Fatigue resistance and crack growth performance. *International Journal of Fatigue*, 48:300–307, 2013.

[36] P. Li, D. H. Warner, A. Fatemi, and N. Phan. Critical assessment of the fatigue performance of additively manufactured Ti-6Al-4V and perspective for future research. *International Journal of Fatigue*, 85:130–143, 2016.

[37] S. Lou, X. Jiang, W. Sun, W. Zeng, L. Pagani, and P. J. Scott. Characterisation methods for powder bed fusion processed surface topography. *Precision Engineering*, 57(August 2018):1–15, 2019.

[38] Eric Wycisk, Andreas Solbach, Shafaqat Siddique, Dirk Herzog, Frank Walther, and Claus Emmelmann. Effects of defects in laser additive manufactured Ti-6Al-4V on fatigue properties. *Physics Procedia*, 56(C):371–378, 2014.

[39] K Mutombo and P Rossouw. Effect of Pickling Solution on the Surface Morphology of Ti-6Al-4V alloy Investment Cast. *ITA Conference*, pages 6–11, 2011.

[40] Guoying Dong, Julien Marleau-Finley, and Yaoyao Fiona Zhao. Investigation of electrochemical post-processing procedure for Ti-6Al-4V lattice structure manufactured by direct metal laser sintering (DMLS). *International Journal of Advanced Manufacturing Technology*, 104(9-12):3401–3417, 2019.

[41] R I M Asri, W S W Harun, M A Hassan, S A C Ghani, and Z Buyong. A review of hydroxyapatite-based coating techniques : Sol - gel and electrochemical depositions on biocompatible metals. *Journal of the Mechanical Behavior of Biomedical Materials*, 57:95–108, 2016.

[42] R. Ramakrishna, J. Mayer, E. Wintermantel, and Kam W. Leong. Biomedical applications of polymer-composite materials: a review. *Comosites Science and Technology 61 (2001)1189-1224*, 2:861–865, 2002.

[43] Umar Ali, Khairil Juhanni Bt Abd Karim, and Nor Aziah Buang. A Review of the Properties and Applications of Poly (Methyl Methacrylate) (PMMA). *Polymer Reviews*, 55(4):678–705, 2015.

[44] Hamizah Abdul Samad and Mariatti Jaafar. Effect of polymethyl methacrylate (PMMA) powder to liquid monomer (P/L) ratio and powder molecular weight on the properties of PMMA cement. *Polymer - Plastics Technology and Engineering*, 48(5):554–560, 2009.

[45] Xuelin Li and Igor Zhitomirsky. Deposition of poly(methyl methacrylate) and composites containing bioceramics and bioglass by dip coating using isopropanol-water co-solvent. *Progress in Organic Coatings*, 148(May):105883, 2020.

[46] Samarah V. Harb, Andressa Trentin, Mayara C. Uvida, Marina Magnani, Sandra H. Pulcinelli, Celso V. Santilli, and Peter Hammer. A comparative study on PMMA-TiO2 and PMMA-ZrO2 protective coatings. *Progress in Organic Coatings*, 140(October 2019), 2020.

[47] L. Floroian, C. Samoila, M. Badea, D. Munteanu, C. Ristoscu, F. Sima, I. Negut, M. C. Chifiriuc, and I. N. Mihailescu. Stainless steel surface biofunctionalization with PMMA-bioglass coatings: compositional, electrochemical corrosion studies and microbiological assay. *Journal of Materials Science: Materials in Medicine*, 26(6):10856, 2015.

[48] Zhe Yang, Hongdan Peng, Weizhi Wang, and Tianxi Liu. Crystallization behavior of poly(ϵ-caprolactone)/layered double hydroxide nanocomposites. *Journal of Applied Polymer Science*, 116(5):2658–2667, 2010.

[49] I. Milošev, T. Kosec, and H. H. Strehblow. XPS and EIS study of the passive film formed on orthopaedic Ti-6Al-7Nb alloy in Hank's physiological solution. *Electrochimica Acta*, 53(9):3547–3558, 2008.

[50] Vitali Goriainov, Richard Cook, Jeremy M. Latham, Douglas G. Dunlop, and Richard O.C. Oreffo. Bone and metal: An orthopaedic perspective on osseointegration of metals. *Acta Biomaterialia*, 10(10):4043–4057, 2014.

[51] B. Feng, J. Weng, B. C. Yang, S. X. Qu, and X. D. Zhang. Characterization of surface oxide films on titanium and adhesion of osteoblast. *Biomaterials*, 24(25):4663–4670, 2003.

[52] David M. Dohan Ehrenfest, Paulo G. Coelho, Byung Soo Kang, Young Taeg Sul, and Tomas Albrektsson. Classification of osseointegrated implant surfaces: Materials, chemistry and topography. *Trends in Biotechnology*, 28(4):198–206, 2010.

[53] PenttiTengvallIngemarLundström. ical Considerations of Tita. *Clinical Materials*, 9:115–134, 1992.

[54] K. Anselme. Osteoblast adhesion on biomaterials. *Biomaterials*, 21(7):667–681, 2000.

[55] Barbara D. Boyan, S. Lossdörfer, L. Wang, G. Zhao, C. H. Lohmann, D. L. Cochran, and Z. Schwartz. Osteoblasts generate an osteogenic microenvironment when grown on surfaces with rough microtopographies. *European Cells and Materials*, 6(May 2014):22–27, 2003.

[56] Tadashi Kokubo and Hiroaki Takadama. How useful is SBF in predicting in vivo bone bioactivity? *Biomaterials*, 27(15):2907–2915, 2006.

[57] M. Geetha, A. K. Singh, R. Asokamani, and A. K. Gogia. Ti based biomaterials, the ultimate choice for orthopaedic implants - A review. *Progress in Materials Science*, 54(3):397–425, 2009.

[58] Ajay Kumar Mishra. Sol-gel based nanoceramic materials: Preparation, properties and applications. *Sol-gel Based Nanoceramic Materials: Preparation, Properties and Applications*, pages 1–297, 2016.

[59] Dongwoo Khang, Jing Lu, Chang Yao, Karen M. Haberstroh, and Thomas J. Webster. The role of nanometer and sub-micron surface features on vascular and bone cell adhesion on titanium. *Biomaterials*, 29(8):970–983, 2008.

[60] J. Karch, R. Birringer, and H. Gleiter. Ceramics ductile at low temperature. *Nature*, 330(6148):556–558, 1987.

[61] A. Ibrahim, R. S. Lima, C. C. Berndt, and B. R. Marple. Fatigue and mechanical properties of nanostructured and conventional titania (TiO2) thermal spray coatings. *Surface and Coatings Technology*, 201(16-17):7589–7596, 2007.

[62] M. Shirkhanzadeh. XRD and XPS characterization of superplastic TiO2 coatings prepared on Ti6Al4V surgical alloy by an electrochemical method. *Journal of Materials Science: Materials in Medicine*, 6(4):206–210, 1995.

[63] M. Shirkhanzadeh and S. Sims. Immobilization of calcium phosphate nano-clusters into alkoxy-derived porous TiO2 coatings. *Journal of Materials Science: Materials in Medicine*, 8(10):595–601, 1997.

[64] Hae Won Kim, Hyoun Ee Kim, Vehid Salih, and Jonathan C. Knowles. Hydroxyapatite and titania sol-gel composite coatings on titanium for hard tissue implants; mechanical and in vitro biological performance. *Journal of Biomedical Materials Research - Part B Applied Biomaterials*, 72(1):1–8, 2005.

[65] Å K. Jämting, J. M. Bell, M. V. Swain, L. S. Wielunski, and R. Clissold. Measurement of the micro mechanical properties of sol-gel TiO2 films. *Thin Solid Films*, 332(1-2):189–194, 1998.

[66] Hamizah Abdul Samad and Mariatti Jaafar. Polymer-Plastics Technology and Engineering Effect of Polymethyl Methacrylate (PMMA) Powder to Liquid Monomer (P/L) Ratio and Powder Molecular Weight on the Properties of PMMA Cement Effect of Polymethyl Methacrylate (PMMA) Powder to Liquid Monomer (P/L) . 2009.

[67] Michelina Catauro and Stefano Vecchio Ciprioti. Sol-Gel Synthesis and Characterization of Hybrid Materials for Biomedical Applications BT - Thermodynamics and Biophysics of Biomedical Nanosystems: Applications and Practical Considerations. pages 445–475. Springer Singapore, Singapore, 2019.

[68] Hae Won Kim, Young Hag Koh, Long Hao Li, Sook Lee, and Hyoun Ee Kim. Hydroxyapatite coating on titanium substrate with titania buffer layer processed by sol-gel method. *Biomaterials*, 25(13):2533–2538, 2004.

[69] D. B. Haddow, S. Kothari, P. F. James, R. D. Short, P. V. Hatton, and R. Van Noort. Synthetic implant surfaces: 1. The formation and characterization of sol-gel titania films. *Biomaterials*, 17(5):501–507, 1996.

[70] I. A. Ovid'ko and A. G. Sheinerman. Micromechanisms for improved fracture toughness in nanoceramics. *Reviews on Advanced Materials Science*, 29(2):105–125, 2011.

ETH

Eidgenössische Technische Hochschule Zürich
Swiss Federal Institute of Technology Zurich

Eigenständigkeitserklärung

Die unterzeichnete Eigenständigkeitserklärung ist Bestandteil jeder während des Studiums verfassten Semester-, Bachelor- und Master-Arbeit oder anderen Abschlussarbeit (auch der jeweils elektronischen Version).

Die Dozentinnen und Dozenten können auch für andere bei ihnen verfasste schriftliche Arbeiten eine Eigenständigkeitserklärung verlangen.

Ich bestätige, die vorliegende Arbeit selbständig und in eigenen Worten verfasst zu haben. Davon ausgenommen sind sprachliche und inhaltliche Korrekturvorschläge durch die Betreuer und Betreuerinnen der Arbeit.

Titel der Arbeit (in Druckschrift):

Effect of Surface Modifications on the Fatigue Performance of Additively Manufactured Ti-6Al-4V Miniature Tensile Specimens Used in Lattices for Orthopaedic Implants

Verfasst von (in Druckschrift):
Bei Gruppenarbeiten sind die Namen aller Verfasserinnen und Verfasser erforderlich.

Name(n):   **Vorname(n):**

Markovic   Patrik

Ich bestätige mit meiner Unterschrift:
 - Ich habe keine im Merkblatt „Zitier-Knigge" beschriebene Form des Plagiats begangen.
 - Ich habe alle Methoden, Daten und Arbeitsabläufe wahrheitsgetreu dokumentiert.
 - Ich habe keine Daten manipuliert.
 - Ich habe alle Personen erwähnt, welche die Arbeit wesentlich unterstützt haben.

Ich nehme zur Kenntnis, dass die Arbeit mit elektronischen Hilfsmitteln auf Plagiate überprüft werden kann.

Ort, Datum   **Unterschrift(en)**

Birmensdorf, 30.03.2021

Bei Gruppenarbeiten sind die Namen aller Verfasserinnen und Verfasser erforderlich. Durch die Unterschriften bürgen sie gemeinsam für den gesamten Inhalt dieser schriftlichen Arbeit.